UNIVERSITÀ POLITECNICA DELLE MARCHE

DIPARTIMENTO SCIENZE DELLA VITA

E DELL'AMBIENTE

Corso di Laurea Magistrale in Biologia Marina

Effects of different spectral quality and temperature levels in the symbiotic coral

Cladocora Caespitosa

Effetti di diverse qualità di spettri e livelli di temperatura nel corallo simbionte

Cladocora Caespitosa

Tesi di Laurea Magistrale

di: Elisa Orlandini

Relatore:

Chiar.ma Prof.ssa Cristina Di Camillo

Correlatori:

Chiar.ma Prof.ssa Caterina Gerotto
Chiar.mo Prof. Carlo Cerrano

Sessione Autunnale Ottobre

Anno Accademico 2023/2024

Summary

Riassunto

Il corallo *Cladocora caespitosa* è una specie endemica del Mar Mediterraneo adattata a vivere a profondità diverse (7-15m) e a fluttuazioni di temperatura stagionali (13°C – 23°C). In questo progetto di tesi si è voluto analizzare gli effetti di una qualità di luce al di fuori del range della PAR (Phosynthetic Active Radiation) e della temperatura sulla crescita di *Cladocora caespitosa,* verificando se tali fattori influenzino significativamente il suo sviluppo nel tempo. L'obiettivo di questi esperimenti è stato quello di analizzare come *C. caespitosa* e le cellule simbiotiche al suo interno reagissero all'esposizione della luce infrarossa, in un contesto anche di cambiamenti climatici in cui questi potrebbero determinare cambiamenti anche nell'intensità luminosa e conseguenze sulla fenologia dei coralli e la relazione tra corallo e simbionte. In particolare, sono stati condotti due esperimenti, ciascuno dalla durata di due mesi. Il primo prevedeva un tempo di esposizione alla luce di due ore al giorno, mentre il secondo di 10 ore. Il disegno sperimentale ha previsto l'utilizzo di otto vasche totali, ognuna delle quali conteneva tre colonie di *C. caespitosa* posizionate su un supporto in PVC per assicurare un'adeguata esposizione alla luce. La temperatura dell'acqua in quattro di queste vasche sperimentali è stata portata a 20°C, mentre le altre quattro a 23°C. L'illuminazione è stata fornita tramite due lampade LED: una caratterizzata da una lunghezza d'onda compresa tra 500 a 730 nm (PAR+IR), e l'altra caratterizzata invece da una lunghezza d'onda che comprende la luce fotosinteticamente attiva e una percentuale di luce nel blu, a 460nm (PAR). Le vasche di controllo sono state illuminate con solo le lampade PAR, mentre quelle trattate erano caratterizzate da entrambe le tipologie di lampade: PAR e PAR+IR. Le analisi sono state effettuate periodicamente ogni tre settimane, con misurazioni relative alla morfologia e all'efficienza fotosintetica. In particolare, di ogni campione è stata misurata nel tempo l'area, l'altezza, il numero di buds e la concentrazione di cellule simbionti presenti nei loro tessuti. L'efficienza fotosintetica massima al buio (Fv/Fm), il Non-Photochemical-quenching NPQ e il Quantum yield del PSII Y(II) sono stati misurati tramite Pulse Amplitude Modulation (DIVING-PAM). In laboratorio sono state poi estratte le clorofille da campioni prelevati e determinata la loro concentrazione attraverso lo spettrofotometro. Il primo esperimento non ha riscosso risultati significativi, probabilmente per la breve durata di esposizione. Nel secondo invece, con

un’esposizione al LED infrarosso di 10 ore al giorno, non è stata registrata un’inibizione della crescita; al contrario, questa sembra promossa in altezza soprattutto nei campioni appartenenti alle vasche con temperature più alte (23°C). Il numero di buds è promosso invece in tutti i campioni dall’aumento della temperatura, dalle vasche pre-esperimento a 16°C a quelle sperimentali di 20 e 23°C. Questi risultati offrono un punto di partenza per ulteriori indagini volte ad esplorare più in dettaglio la relazione tra Symbiodiniaceae e *C. caespitosa* e la loro capacità di adattamento e crescita a diverse condizioni di illuminazione, comprese quelle al di fuori dal range della PAR.

1. INTRODUCTION

Scleractinia is an order of corals belonging to the class of Hexacorallia. They are commonly known as hard corals for the presence of a calcium carbonate skeleton that they secrete and they are the primary builders of coral reefs. Their evolutionary success is linked to their mutualistic symbiosis with microalgae (belonging to the Symbiodiniaceae family) located within their gastrodermal tissue (Wangpraseurt et al., 2016). In this symbiotic relationship, coral polyps provide essential nutrients such as ammonia and CO_2 to support the microalgae, which in turn it produces oxygen and metabolic by-products through photosynthesis. For instance, although symbiont-bearing corals partly rely on heterotrophic energy via particle and prey capture thanks to presence of the cnidocytes, most of their energy demand is covered by endosymbiotic microscopic dinoflagellate algae of the family Symbiodiniaceae. However, stressors such as increasing temperatures and light intensity can interfere in this delicate balance. Corals are characterized by a high diversity in shape and dimension, and this influence the light absorption that tend to decrease in increasing of dimension of the colony (Stambler & Dubinsky, 2005; Wangpraseurt et al., 2016). Moreover, they thrive in a wide range of depths (e.g. shallow-water and mesophotic corals) exposing them to varying levels of irradiance. Consequently, corals possess mechanisms to regulate and modulate the penetration of light through their tissues (Bhagooli & Hidaka, 2004).

Even if sunlight is crucial for photosynthesis and the survival of both the coral and its endosymbiont, excessive photosynthetically active radiation (PAR) can lead to photoinhibition: a process where the photosynthetic capacity and efficiency decline due to light stress (Bhagooli & Hidaka, 2004). To face this phenomenon, corals are known to have systems with which they can protect themselves from excessive radiation or lack of light. The harvest of light is a very dynamic process that create microenvironmental optical controls to protect the relationship with the symbiont (Wangpraseurt, Larkum, et al., 2014)

Various studies have been conducted in which it has been analyzed their behavior in relation with different spectrum of light, particularly with Far Red light and UV, but little is known about what happens when they are illuminated by infrared light. Corals can harvest light in many ways: they can modulate the light penetrating through the tissue by retracted their tentacles, but, because they are unable to move from the source of light, there are other

mechanisms involved in modulating light such as the role of pigments, the tissue and the skeleton that can backscatter light in the tissue. Another important role is played by the symbionts that can try to fight the excess of light and in the worst case they can be expelled by the host leading to coral bleaching (Bhagooli & Hidaka, 2004).

Various studies have been concentrated in determining the optical proprieties of corals focusing on the skeleton's optical proprieties (Enríquez et al., 2005;Terán et al., 2010;Marcelino et al., 2013), while others investigated the role of the tissue and the fluorescent proteins resident in there (Salih et al., 2000;D'Angelo et al., 2008; Wangpraseurt, Larkum, et al., 2014).

Optical proprieties quantify the probability of light absorption and the direction of light scattering. It's important therefore to nominate factors such as absorption coefficient μ_a and scattering coefficient μ_s which can describe mathematically the modulation of light harvesting and scattering of light through the tissue and the skeleton (Wangpraseurt et al., 2016). Understanding how light moves through different parts of coral skeleton and tissue can help us to make predictions of light exposure at the level of individual symbiont cells within the coral tissue under various regimes of incident solar radiation. Therefore, quantifying the optical properties of corals has a significant implication for understanding the ecophysiology of symbionts within their host (Wangpraseurt et al., 2016).

1.1 Harvesting light in Scleractinian

1.1.1 Fluorescent proteins

In 1994, Chow and Osmond proposed that reduced efficiency is a crucial response for maintaining a balance between photoprotection, where excess energy is dissipated as heat, and the potential damage that sunlight can inflict on photosystem II proteins. Therefore, corals have developed pathways to protect themselves from excessive light exposure: host's pigments play a vital role in shielding endosymbionts from high light levels and in optimizing light conditions for shade-adapted corals and can absorb light in the visible and UV range (Galindo-Martínez et al., 2022; Salih et al., 2000). These proteins can be classified by their spectral properties into fluorescent proteins (FPs) where we find cyan fluorescent proteins (CFPs), green fluorescent proteins (GFPs), red fluorescent proteins (RFPs), and non-fluorescent proteins CPs. While, based on their regulation properties, host pigments can be categorized as light-induced or constitutive, depending on whether transcription of their respective genes is induced by blue light or not. Moreover, they can be found distributed above or below the symbiont. They can also be found diffusely, or they can form granules of pigments (Ferreira et al., 2023). Among their various roles, host pigments are particularly important for dissipating light by regulating and altering the light field within tissues and can reemit light at different wavelengths through a process called photoconversion (Ferreira et al., 2023; Galindo-Martínez et al., 2022; D'Angelo et al., 2008). Those kinds of proteins are characterized by spectral properties allowing them to intervene in regulating the light exposure (Stephens S. Ban, 2014). Salih and other researchers discovered that fluorescent proteins (FPs) are strategically positioned above endosymbionts to provide photoprotection against excessive sunlight. Nevertheless, in shaded environments, FPs are located below or among the endosymbionts to enhance photosynthesis through two main mechanisms: wavelength transformation (where a special kind of FPs are able to convert actinic light into non-actinic light) and back-scattering. FPs are crucial in reducing the risk of irreversible photoinhibition, photooxidation, and subsequent coral bleaching. This allows coral polyps to optimize tissue photosynthetic activity enhancing the survival of the host (Salih et al., 2000). The production of fluorescent proteins to enhance or dissipate light energy is therefore also viewed as a strategy to harvesting light in heterogenous environments (Salih et al., 2000).

Fluorescent proteins (FPs) can vary not only between different coral species but also among individuals within the same species. This variability can be attributed to phenomena such as polyphenism or polymorphism. Polymorphism involves genetic differences at the genome level, resulting in different sets of genes, whereas polyphenism is characterized by variations in gene expression regulated by environmental factors, including light (Ferreira et al., 2023; D'Angelo et al., 2008). The intensity and spectrum of light plays crucial roles in influencing the gene expression of fluorescent proteins. A study carried out by D'Angelo et al. in 2008 demonstrated that hermatypic corals exposed to blue light (200 μmol $m^{-2}s^{-1}$) exhibited higher concentrations of GFP-like proteins, while those under red light showed pigments belonging to a low-threshold category (present in higher concentrations under low photon flux) with significant gene expression (≥ 50%) specifically in response to green light stimulation. Therefore, the expression of fluorescent proteins increases progressively from red to blue light wavelengths. The concentration of these proteins in coral tissue was observed to increase with a higher light flux of 80 μmol $m^{-2}s^{-1}$ and saturate around 400μmol $m^{-2}s^{-1}$. Coral pigments not only play a photoprotective role but also likely influence the interaction with the symbiont, potentially enhancing the photosynthetic rate (D'Angelo et al., 2008).

Another aspect to consider is the spatial arrangement of fluorescent proteins (FPs), as it significantly influences their effectiveness. FPs may be distributed in various patterns such as homogeneous distribution throughout the tissue, concentrated at the tentacle tips, within the oral cavity of the polyp, along the colony margin, in the ectoderm, in the gastroderm, or around the symbionts (Ferreira et al., 2023). The location of pigments is different between shallow-water corals and mesophotic/deep corals. In the first one we might often find pigments located in the ectoderm and in the gastrodermis above the symbiont, while in mesophotic and deep-water corals they are generally more distributed below or around the symbionts. Pigments can also be found aggregated in granules or with a more diffused distribution (Ferreira et al., 2023). Based on the pattern of distribution of FPs, corals exhibit different light scattering granules tend to show a more diffuse light scattering which bring light closer to the coral tissue surface and a more rapid vertical light attenuation from the coral surface towards deeper layers than what we can observed in corals with diffuse-distributed FPs. These diverse spatial arrangements highlight how FPs strategically optimize

light management within coral tissues, influencing both photoprotection and photosynthetic efficiency (Ferreira et al., 2023).

In mesophotic environments, corals experience less intense environmental variations with temperature, wave activity and irradiance. For those mesophotic corals it is important to be able to optimize the light harvesting and coral photosynthesis in a habitat where only the ~3-10% of the surface irradiance will arrive shifted towards a blue wavelength. Mesophotic corals show lower energy requirements and an increased tendency on heterotrophic feeding, a change in colony morphology towards a more flattened shapes, and an more space between branches in a way that likely reduces self-shading and increases light harvesting. Optimization of light harvesting is attributed to host pigments mainly due to their relative abundance even in mesophotic habitats, but science evidence is still lacking. Corals can also be characterized by photoconvertible fluorescent proteins (pcRFPs) which are immature green-emitting chromophore that undergoes irreversible photoconversion from green to red emission upon exposure to UV radiation (~390 nm). It has been demonstrated that corals with pcRFPs had a greater survival rate in aquaria after extended low blue light treatment, compared to their non fluorescent counterparts which showed 100% mortality (Smith et al., 2017). The suggestion was that pcRFPs in corals enable the transformation of blue-green wavelengths to orange-red light which penetrates deeper in the tissue, and this is possible due to a mechanism of energy transfer called FRET between green and orange subunits of pcRFPs (Smith et al., 2017). Fluorescence Resonance Energy Transfer (FRET) is an energy transfer process from an excited donor chromophore to an acceptor chromophore via intermolecular long-range dipole-dipole coupling (Ferreira et al., 2023). Blue light is rapidly absorbed by the chlorophyll pigment of the symbiont while orange-red light doesn't get absorbed is such efficiency way. This difference makes the orange-red light able to penetrate deeper into coral tissue where it can be absorbed by the dinoflagellate found in deeper layers of the tissue. PcRFPs corals, transforming blue light into orange, increase the time of photons in the tissue enhancing the chances for the symbionts to capture photons for photosynthesis (Ferreira et al., 2023; Wangpraseurt, Tamburic, et al., 2014).

1.1.2 Backscattering of the skeleton

Hard-bodied corals form a skeleton composed of solid aragonitic $CaCO_3$. Studies on skeletal characteristics increased over the years since the discovery of density bands and their potential as proxy records of environmental change. Those bands are the results of changes in the carbonate deposition rate during alternating periods of slow and rapid growth and provide therefore historical record on the coral's growth (Bucher et al., 1998). The skeleton's density is related to the material of which the skeleton is made and the number and volume of skeletal voids (porosity), which are empty cavities within the coral skeleton typically lined by living tissue (Bucher et al., 1998). Density and porosity can vary between corals (intra and inter-specific variations), e.g. massive corals are generally less dense (and more porous) than foliaceous corals, and for some species density increase with increasing of depth. Those differences might be due to trade-offs between skeletal density and other factors such as feeding strategies or competition for space(Hughes, 1987).

It is well-known the importance of the calcified skeleton in backscattering and lateral light transfer within coral structures (Wangpraseurt, Larkum, et al., 2014). The skeleton acts as a Lambertian-like diffuser redirecting photons back into the tissue and enhancing their pathway of photons. This led to an enhancement in tissue irradiance (three time more elevated than downwelling irradiance) with the result in an enhancement in phosynthetic efficiency, in the growth of the coral and its calcification rate (Wangpraseurt, Larkum, et al., 2014; Enríquez et al., 2017). Multiple scattering maximizes light absorption capacity even with low pigment concentrations and reduces corals self-shading in low-light environments. The optical properties of the skeleton depend significantly on its morphology and density; thicker corallites guide more light into the coral layers, whereas denser structures facilitate diffuse backscattering (Wangpraseurt et al., 2012). The animal tissue of corals is practically transparent, allowing light to penetrate deeply. The skeleton, on the other hand, is a white, highly scattering structure that diffuses light. The unicellular algae, which are about 10 μm in diameter, are primarily responsible for most of the optical absorption within this structure but it has been observed that the skeleton plays a major role in the illumination of the symbionts as well (Terán et al., 2010). To quantify photon refraction within tissue layers and the skeleton, Mathematical and physical approaches such as the Coral Model and Monte Carlo Simulation, were used to model how light travels through tissues (Terán et al., 2010;

Wangpraseurt et al., 2016). These models explore the relationship between light and the skeleton, providing a generalized representation of coral structures and elucidating qualitative light trends. With this model the researchers investigated and calculated the fraction of the incident light absorbed by the unicellular algae within the tissue layer and the reaction in relation the skeleton. In studies of flat layers (only coenosarc, i.e., coral living tissue with symbiotic algae), it was found that light absorption at each site is linked to local light intensity, which shows a rapid decline within the layer. The upper face receives nearly twice as much light as the rear, with upper cells absorbing light and shading lower cells. Cells near the upper face absorb some light, shading those near the lower end. Consequently, the average absorption per particle is less than that of an isolated particle, resulting in an enhancement factor $\varepsilon < 0.7$ (light environment is enhanced when $\varepsilon > 1$ and reduced when $\varepsilon < 1$). This inefficiency indicates that a flat, well-pigmented layer of coral tissue is not ideal for light harvesting because the light is not evenly distributed. However, placing a flat coral skeleton behind the absorbing layer, known as the "flat coral model," changes this dynamic. With normal light incidence, the algae layer absorbs 74% of the light. The self-shadowing effect decreases, increasing the total absorption of the layer, with an enhancement factor of $\varepsilon = 0.96$. This is because the transmitted light is diffusely reflected by the substrate and passes through the layer again, increasing the absorption. This configuration is clearly better for light harvesting. Finally, they considered a schematic representation of a coral model (non-flat representation) and in this case 87% of light was absorbed by the algae and the ε factor was equal to 1.12. These findings suggest that, despite the high surface density of cells, the light field within the animal tissue layer is stronger than outside the structure. Furthermore, absorption maps from Monte Carlo calculations show that the light field is very uniform within the animal tissue. With these findings they demonstrated the high efficiency of the coral model as a light-harvesting structure. These results highlight the significance of the skeleton in shaping the light environment for the symbionts. Moreover, thanks to Monte Carlo models it was possible to demonstrate the different characteristics of the skeleton about their scattering and absorption abilities: there are skeletons with a much higher scattering coefficient and skeleton with a lower coefficient. Evidence shows that the low reduced scattering and absorption coefficients of the skeleton can facilitate efficient light propagation through the skeletal matrix reaching a homogenization of light propagation. This model and simulation experiments illustrated the benefit of such skeletal light

propagation: light can travel across polyps' walls, through the corallite skeleton and illuminate tissue areas not directly exposed by the sun leading to a more homogeneous light exposure of the coral (Terán et al., 2010; Wangpraseurt et al., 2016). For instance, calcium carbonate skeletons backscatter light back to the algae amplifying light available to the symbiont by 3-20 times to incident irradiance. Scattering makes otherwise shaded symbionts to be able to get reached by photons and use it for photosynthesis. It has been demonstrated that this process is more likely to happen in corals with low skeleton scattering coefficient, compared to those with a higher scattering coefficient (Marcelino et al., 2013). This solar energy collection strategy works effectively in healthy corals which exhibit faster growth rates, but it can be detrimental for corals with low scattering coefficient during bleaching episodes because it makes them more susceptible and thus can enhance the bleaching response. In such scenarios, it becomes crucial to consider potential strategies to face these stressful conditions. For example, certain corals can enhance their calcareous skeletal structures by incorporating organic compounds to add pigmentation. Additionally, skeletons can become less reflective when hosting endolithic communities of phototrophic microorganisms (Terán et al., 2010; Marcelino et al., 2013).

It's not just the scattering coefficient that characterized the skeleton, but also its shape has a great importance in their optical proprieties and macrostructures such as coenosteum, chalices and septa play an important role in the shaping of the algal light environment. Coenosteum is the porous skeleton that links polyp corallites (the skeleton of each individual coral polyp) within a colony and it is secreted by the coenosarc (thin sheet of tissue that inter-connected neighboring polyps of the colony). Each polyp resides in the calyx of each corallite and the space within the calyx is called calice, or chalice. The calyx is surrounded by a wall called the theca which is transected by vertical plates called septa (Fig. 1.1) (NOAA). Corals are characterized by a wide range of shapes that influence their optical proprieties, e.g. in plocoid corallite morphology all individual polyps have their own wall and in phaceloid corals the separate walls of each polyps are tall and tubular. Meanwhile, in cerioid morphology multiple corallites share a single wall and in meandroid morphology polyps share corallite walls and form valleys (Fig. 1.2) (NOAA).

Lowest light enhancement factor LEF has been found in more primitive corals with a phaceloid[1] (Fig 1.2) colonial growth form in which each polyp has an independent light field, while the higher LEF was found in highly integrated flat colonies with the presence of coenosteum, fundamental for the colonial integration because it allows a continuum gastrovascular cavity throughout the colony. The comparison of how, with different skeleton structure, light is scattered, is at the base of the hypothesis for why skeletons that are highly effective at scattering light can sustain more productive holobionts, with higher growth rates and greater competitive ability for space; while organisms with less efficient light-scattering structures may develop robust holobionts, but with reduced productivity and growth rates. Skeleton's capacity to scatter light can potentially sustained two optical proprieties of the holobiont. In one side, the backscattering at the skeleton layers could reduce the costs in harvesting light and therefore it could support the holobiont production and growth in nutrient limited conditions. On the other site, this characteristic could also intervein in reducing the self-shading caused by the host pigments presence (Enríquez et al., 2017). In fact, based on their distribution or organization, host pigments can contribute to the self-shading of coral's tissue. As it will be explained in the following pages, they can be found organized on granules or in a diffuse was, influencing the degree of shading throughout the tissue. Also, they can be found above or below symbionts, which will determinate a certain degree of shadow to the photosynthetic algae (Ferreira et al., 2023). These two important points (reducing self-shading and promote growth in nutrient limited conditions) could have been at the base of the origin of modern Scleractinia reef-builders (Enríquez et al., 2017).

While multiple light scattering by the white skeleton produces diffuse light leading to all the benefits for the host and the symbionts mentioned in this chapter (reducing of pigments self-shading, enlarging optical path), this process can be compromised by the presence of endolithic organisms near the skeletal surface that affect pigment absorption and modifies the light environment of the symbionts inside the tissue (Galindo-Martínez et al., 2022).

[1] *Cladocora caespitosa* (Linnaeus, 1767) shows this kind of morphology

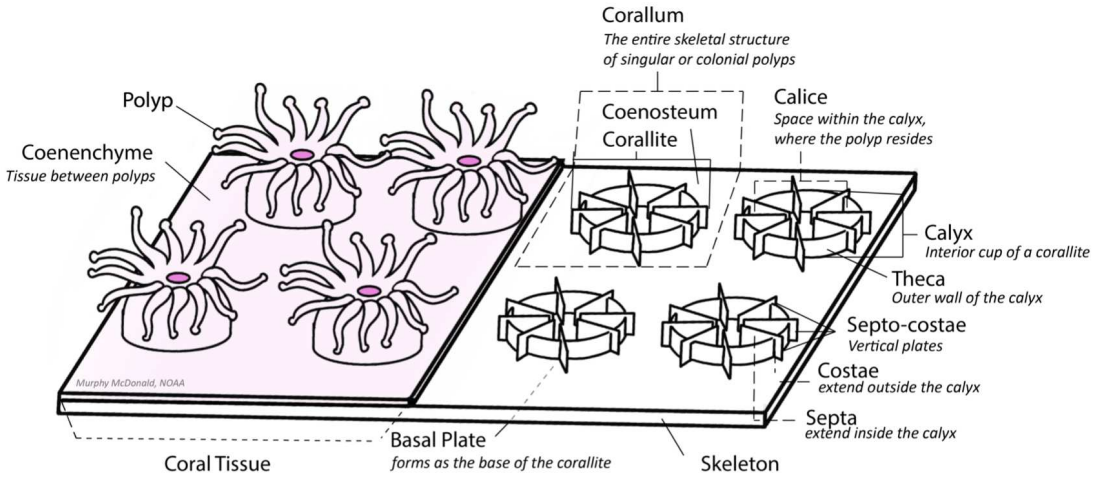

Figure 1.1 Coral skeleton anatomy. Credits: Murphy McDonald, NOAA

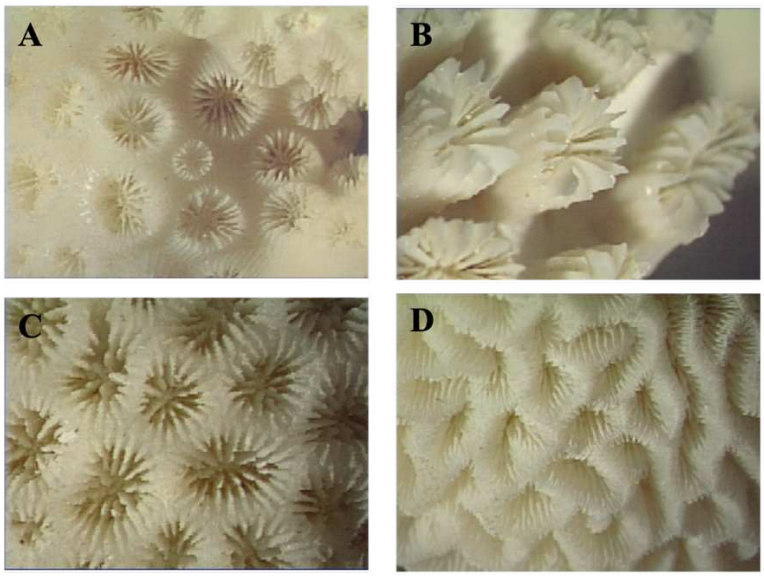

Figure 1.2 A)Plocoid corallite morphology; B)Phaceloid corallite morphology; C) Cerioid corallite morphology and D) Meandroid corallite morphology. Credits: Murphy McDonald, NOAA

1.1.3 Light transfer within corals' tissue

If the role of the skeleton has been well-studied and investigated, the role of the tissue in harvesting light is yet little known for aquatic plants and animals, while it's well known what the tissue can do in terrestrial plants in absorbing and redirecting light (Wangpraseurt et al., 2012). Further studies would lead to the hypothesis that coral tissues can employ similar optical mechanisms as plant leaves, where strong scattering of light within the plant tissue enhances fluence rate and maximized photosynthesis (Wangpraseurt et al., 2016). In most of the studies mentioned in the chapter 1.1.2, researchers assumed no tissue scattering or that the refractive index was comparable to water (Terán et al., 2010). It is indeed possible that skeleton scattering plays a major role in redistribute light in corals where tissue is "thin" and structurally simple, while in other corals characterized with highly developed and "thick" tissues, tissue might be involved in the scattering of the light (Wangpraseurt et al., 2016). Corals are characterized by different layers of tissues and each of them have different composition which can affect the light propagation (Fig 1.3). Mucus layer for example is rich in proteins and sugars affecting the refraction index of light and in the same way mesoglea is rich in lipids which again affect the refraction index of light propagation (Wangpraseurt, Tamburic, et al., 2014). It has been observed that the scalar irradiance, meaning the total amount of light energy available in all direction (upward, downward and laterally) at a given point in coral tissue, differs based on the different typology of tissue. For instance, in Faviid corals under excess levels of incident irradiance, symbionts in aboral tissue layers (overlying the basal floor of the polyp) were able to use in a much more efficient way the limited light that reaches them compared to dinoflagellate algae in oral tissue layers, which were strongly photoinhibited under the same levels of incident irradiance due to the local enhancement of light irradiance caused by the backscattering phenomena. In faviid coral we have therefore a light gradients and optical shelter for the symbionts in aboral tissue, which can be useful during periods of excess radiation (Wangpraseurt et al., 2016). Moreover, it has been observed that scalar irradiance was much higher over the polyp tissue than over coenosarc tissue (the living tissue overlying the stony skeletal material) explained by the presence of host pigments concentrated in the polyp mouth that reflect, fluoresce, and scatter light. (Wangpraseurt et al., 2012). In this study the researchers wanted to test different light regime to which coral might be exposed to provide a basis for future investigations on

microenvironmental optical controls of coral photo- and stress physiology. They investigated in the enhancement of scalar irradiance in different tissue (polyp and coenosarc) and with different regime of incident light: PAR (photosynthetically active radiation) and NIR (near infra-red radiation). They demonstrated an enhancement of scalar irradiance over incident irradiance (radiations that hit a specific area or surface) of about ~180% for PAR and ~250% for NIR, supposedly due to the lack of pigments that absorb efficiently those wavelengths. The difference between coenosarc and polyp tissue nominated earlier happens when corals is illuminated with both PAR and NIR . These Authors found also a constant linear relationship between PAR at the tissue-skeleton interface and incident PAR demonstrating that photons are absorbed before they get scattered by the skeleton: lower tissue are found in more light-limiting conditions than surface tissues which are much more affected by irradiance. This means that tissue itself can contributes to the high efficiency of light absorption (Wangpraseurt et al., 2012). It also has been observed that thick-tissue corals can also provide shelter from light environments for resident symbionts harboring optical microniches in according to what had been proposed years before: thick-tissue corals survive stress events better than thin-tissue ones (Loya, 2001).

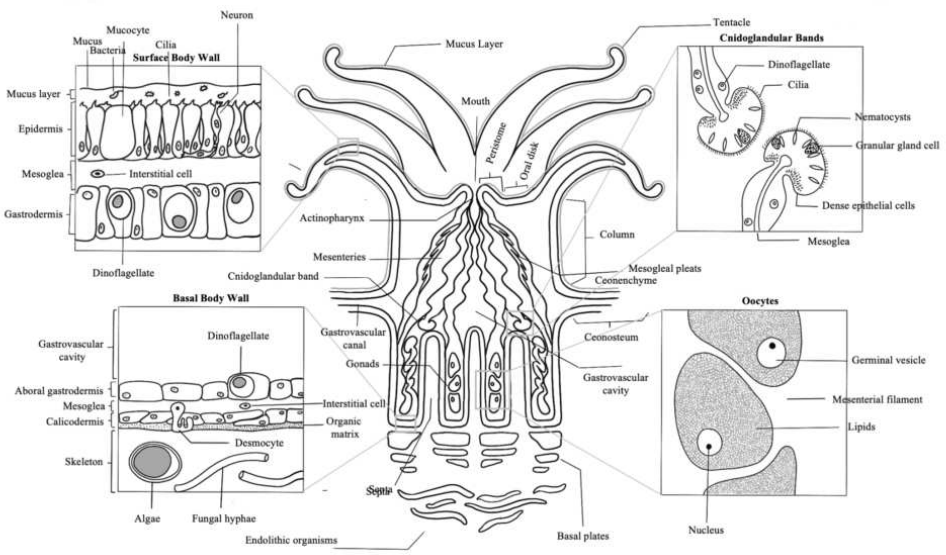

Figure 1.3 Coral polyp anatomy diagram. Credit: Murphy McDonald, NOAA

Scalar irradiances change between the polyp tissue and the coenosarc tissue but it's not the only variation of light we can find; it has been also demonstrated the so-called process of later light transfer by the researchers Wangpraseuirt et al. in 2014. "Latera light transfer" is a term that indicate a new mechanism by which light is redistributed over the coral colony and it seems that optical proprieties of coral's tissue play an important role in this process and it might explain the high photosynthetic efficiency of corals. Specifically, an enhancement of light in upper layers than in lower layers of tissue was observed, which is caused by optical microniches within the coral tissue suggesting that the scattering we thought happening only at the skeleton level, it is present also in tissue level with evidence that lateral light transfer affects coral photosynthesis in tissue areas that are far from the direct source of light. This led to the conclusion that there is a distribution of solar radiation over the coral topography that enables the efficient use of light by the symbiotic algae (Wangpraseurt, Larkum, et al., 2014). With a laser-beam Wangpraseurt et al. (2014) evaluated the diffusion of the light from the input both in red (636nm) and in near-infrared (785nm) light. NIR was the best source of light in terms of being redistributed laterally and homogeneously, while light from the red spectrum was diffused more heterogeneously within the tissue, however it has been highlighted no difference in light distribution between the coral tissue and the skeleton which led to the conclusion that with NIR the lateral propagation is mainly due to the role of skeleton. Significant differences were found with red light (interacting with host, zooxanthellae pigments and cell walls) in which has been hypothesized that tissue optical proprieties influence more the light distribution, and a less important role is attributed at the skeleton. These mechanisms result to be optimal in those light-limiting conditions in which lateral transfer of light can allow the holobiont to collect and trap as much as photons as possible. On the other hand, this mechanism can also damage the organism when it is over exposed to high irradiance (e.g. low tide condition led to a much higher exposure) and for this reason it evolved a physical mechanism of photoprotection —i.e., physical contraction of the tissue— to protect itself from an over exposure to sunlight. Incident light can be more diffuse through an expanded tissue, while in the case the tissue is contracted, the lateral light transferring is much more inefficiently protecting the algae from an excess of light (Wangpraseurt, Larkum, et al., 2014; Ferreira et al., 2023).

The expansion and contraction of coral tentacles are also influenced by the concentration of symbiotic algae. Corals with dense populations of these algae tend to keep their tentacles expanded continuously over the day (diurnal behavior), maximizing light absorption for photosynthesis (Levy et al., 2003). On the other hand, corals with fewer symbionts often retract their tentacles during the day and expand them at night to capture prey (nocturnal behavior). This behavior may be also related to the tentacle morphology and function. Tentacles with fewer symbionts often have a finger-like shape (e.g. *Plerogyra sinuosa*), suitable for prey capture but less effective for light absorption, leading to nocturnal expansion. Conversely, flower-shaped tentacles with high symbiont densities expand during the day to maximize light absorption (e.g. *Goniopora lobata*) (Fig. 1.4). Expanding tentacles with low symbiont numbers during the day can be energetically expensive and it might reduce photosynthetic efficiency due to light scattering. For example, *Montastrea cavernosa* has two morphotypes: one with dense Symbiodiniaceae populations remains open during the day, while the other, with fewer zooxanthellae, expands only at night (Levy et al., 2003).

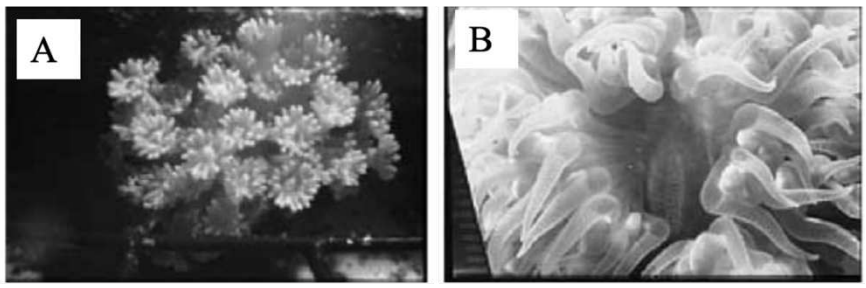

Figure 1.4 A) Flower-shape tentacles of G. lobata *and B) finger-shape tentacles of* P. sinuosa. *Credits: (Levy et al., 2003)*

Fluorescence techniques (FRRF measurements) show that when the tentacles of nocturnal coral species are extended, they scatter some of the incoming light (Levy et al., 2003). This scattering means that less light energy reaches the zooxanthellae. As a result, the ability of chlorophyll to get excited by light decreases, leading to reduced fluorescence (F0 and Fm) and a lower functional absorption cross section of PSII (σPSII), which is a measure of how effectively PSII can absorb light. In nocturnal species, extended tentacles tend to scatter some of the radiation due to the lack of symbionts and thus, less excitation energy reaches the symbiotic algae. The retraction of tentacles, on the other hand, enhances the algae's ability to capture light, maximizes light exposure and increasing the photosynthetic

performance of the algae. Despite this increase in photosynthetic efficiency, the overall efficiency of how absorbed light is used (measured by Fv/Fm) remains constant, indicating that once light is absorbed, it is utilized with the same efficiency regardless of how much light is absorbed (Levy et al., 2003).

Another suggestion is that corals manage light exposure through the expansion and contraction of polyps, altering the concentration of fluorescent pigments in the tissue. High light levels cause polyps to contract, increasing pigment density and forming a protective layer against excessive light (Levy et al., 2003).

Another aspect that needs to be taken in consideration about the contraction and expansion of tissue is that, as mentioned in the chapter 1.1.1, host pigments can be differently distributed among ectodermal and gastrodermal, above or below the symbionts, in granules or in a more diffuse way. Contraction and expansion of the tissue can dynamically change the optical proprieties of the tissue and the arrangement of the host pigments. Together, these characteristics determine the quality and quantity of light that reaches the symbiont available for photosynthesis (Ferreira et al., 2023).

What we can say is that optical properties of tissue affect not only the distribution of light within it, but also the regulation of host pigments and the propagation of their fluorescence and how pigments can influence the Symbiodiniaceae photosynthetic rate. It has already been faced how the thickness of the tissue can influence the light inside the tissue creating sheltered environments (Y. Loya, 2001), and the vertical gradient present in thick-tissue corals. The irradiance that hit the surface layers is attenuate up to more of 10% in the lower layers (Wangpraseurt et al., 2012). Whereas in thin-tissue corals it seems that they are more influenced by the backscattering of the skeleton more than the role of the tissue (Wangpraseurt et al., 2016; Enríquez et al., 2017). Nonetheless much attention should be directed in investigate in more detail the role and the dynamics between skeleton and tissue in harvesting and scattering light in the holobiont.

1.1.4 Spectra of light: PAR, UV, Far-Red and IR

The light environment is very important for the growth, health, and overall functioning of corals. As light penetrate deeper through seawater, it decreases quickly, following the Beer-Lambert law. This reduction in light happens because of the water, dissolved substances, suspended particles, and especially the presence of phytoplankton. This process doesn't affect all wavelengths of light equally. The water acts like a filter, allowing only certain colors to pass through. In the clear, low-nutrient waters around reefs, violet and blue light are absorbed the least, while longer wavelengths are absorbed more. Despite this, corals in these shallow "blue desert" waters can still receive significant amounts of red and UV light (Levy et al., 2003).

Light is characterized by different spectrum with a different nm range. Usually, it can be classified into UV, visible spectrum and infrared. Most of the studies on the effect of light irradiance on corals focused on the visible spectrum in which it is included the PAR (Photosynthetically Active Radiation) spectrum that ranges from 400 to 700 nm and it is crucial for photosynthesis. Absorption of light in the water column is greatest for the long wavelengths (red) while shorter wavelengths penetrate deeply (blue) (Wijgerde et al., 2014). In this spectrum, blue light (450-495 nm) is found to play a key role in coral growth, coloration, and promotes coral and zooxanthellae growth, chl-a content, FPs production and increase photosynthetic rates (Mass et al., 2010). Light spectrum could influence also symbiont density, and it seems that in blue light we might have higher density than when exposed to red light (Wijgerde et al., 2014).

The UV light range from 280-400 nm, and it is strongly absorbed by water meaning that UV light penetrates only the upper layers of water. It can be divided in UVA (315-400 nm), UVB (280-315) and UVC (100-280 nm) (Bracchini et al., 2005). While the attenuation coefficient (measure how quickly light diminishes in intensity as it travels through a medium) for downwelling irradiance and penetration depth varies based on the optical characteristics of the water, UV is generally absorbed at least twice as quickly as PAR. The clear and nutrient-poor waters allow the 1% of surface UVA and UVB radiation to reach depth of up to 12-22 m and 8.4-12 m, respectively. Consequently, shallow tropical corals can experience

prolonged UV exposure affecting reducing growth, DNA damages and ROS formation (Wijgerde et al., 2014).

Water absorbs almost all the infra-red energy from 780nm to 1mm within 10 centimeters of the surface while visible red and far-red light (620 – 750nm) have slightly more energy than invisible infrared radiation and at 15 meters it is generally all absorbed (Boyd, 2014). Red light appears to have negative or neutral effect on coral growth, mitotic division, symbiont concentration and photophysiology (Wijgerde et al., 2014). Some species (e.g. *S. pistillata*) exposed to red light shows a certain degree of necrosis and mortality and a lower zooxanthellae density compared to blue light (Wijgerde et al., 2014).

While there is a lack of studies focused on understanding the effects of the exposure to infrared or far-red spectrum to marine photosynthetic organisms, a greater understanding has been achieved for terrestrial plants exposed to different light regime, including far-red and infra-red light. Red light can influence various processes such as determining the height of the plant but also chlorophyll biosynthesis. Far-red light enhance the flowering of plants and their ratio (red:far-red) influence important factors like stem elongation, leaf expansion and reproductivity process (Paradiso & Proietti, 2022). A reduced ratio R:FR, affects the activity of key enzymes of nitrogen metabolism and the allocation of nutrients to the plant shoot, resulting in a faster development of the aerial part compared to the roots (Paradiso & Proietti, 2022). Some authors have also demonstrated that supplemental far-red light in LED illumination for hydroponic lettuce farms promotes leaf expansion (shade acclimatation response), which is correlated with an increase in canopy size. This allows the plants to capture more light for photosynthesis leading to an overall increase in lettuce biomass (Legendre & van Iersel, 2021). Far-red supplement has also a great importance on the uptake of macro-nutrients (nitrogen, phosphorous, potassium, calcium, magnesium) and micro-nutrients (sulphur, iron, copper, manganese) improving the nutritional value of lettuce plants (Pinho et al., 2017). Regarding IR radiation, it has a powerful effect on stem elongation and the rate of leaf expansion (Pattison et al., 2018) and in other studies it has been demonstrated that IR seems to enhance the secondary metabolism of eggplants through the enhancement of the biosynthesis of specific compounds such as lariciresinol glucopyranoside, a bioactive lignin glycoside with a noteworthy antiviral property enhancing the overall growth of eggplants (Sinanoglou et al., 2019).

All these responses are possible because photosynthetic cells, including corals' symbionts, are characterized by specifics families of photoreceptors able to absorb different wavelength of light. Phytochromes in particular are the photoreceptors responsible for the absorption of red and far-red light determining those responses earlier mentioned (Paradiso & Proietti, 2022). Cyanobacteria are characterized by red-shifted chlorophylls (chlorophyll-f) and phycobiliproteins capable of harvesting near-infrared-radiation at wavelength > 700-760nm (Kühl et al., 2020). Where these specifics pigments are absent (algae and plants), there is a particular chemical interaction between two chlorophylls that can expand the absorption spectra to wavelength > 700nm (Kosugi et al., 2024).

1.2 The Mediterranean pillow coral: *Cladocora Caespitosa* (Linnaeus, 1767)

Cladocora caespitosa (Linnaeus 1767) is a colonial zooxanthellate scleractinian characterized by phaceloid colonies, with no colonial integration and where each polyp is characterized with an independent light field and a low value of light scattering (Enríquez et al., 2017). It is endemic to the Mediterranean Sea and recognized as one of the most significant reef-building species of the area (Roveta et al., 2023). This coral species thrives in a variety of environmental conditions, from relatively dark conditions, down to 40 meters depth or in very turbid water, to well-lit shallow-water habitats (Hoogenboom et al., 2010). The morphology and spatial development of *C. caespitosa* colonies are influenced by environmental factors such as hydrodynamics, substrate type and seafloor topography (Roveta et al., 2023). Colonies exhibit two primary types of distributions: beds and banks (Fig 1.5). Beds are characterized by numerous distinct subspherical colonies, as observed in places like Gulf of Trieste. In contrast, banks consist of larger colonies that can reach several decimeters in height and cover multiple square meters (Kersting et al., 2023; Chefaoui et al., 2017). *C. caespitosa* is a long-living, slow-growing species characterized with a low recruitment rate and high juvenile mortality. These traits make *C. caespitosa* highly vulnerable to threats including invasive species but also eutrophication, pollution, trawling and dredging, and increasing in sedimentation rate. For these reasons, its distribution is now very limited to specific regions of the Mediterranean Sea (Roveta et al., 2023). Given its critical role as an ecosystem engineer and its rapid decline and low recovery capability, *C. caespitosa* is listed as Endangered on the IUCN Red List for the Mediterranean region (Casado de Amezua et al., 2015).

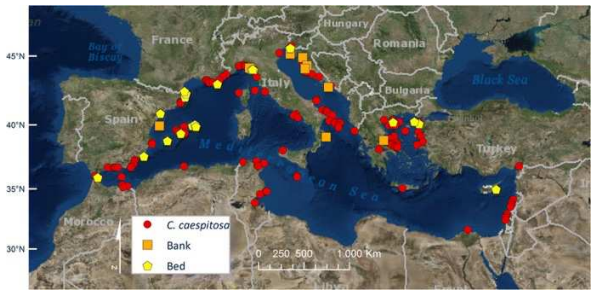

Figure 1.5 Occurence of Cladocora caespitosa *(red circles) and the two type of assemblages analyzed: banks (orange squares) and beds (yellow pentagons)* (Chefaoui et al., 2017). Records of *C. caespitosa* from north-central Adriatic sea (i.e., Riviera del Conero, Grottammare, AMP Torre del Cerrano, Costa dei Trabocchi) are missing in this map.

1.2.1 Feeding strategy and coral growth

Cladocora caespitosa is a zooxanthellate coral, meaning that they rely both on the secondary products of Symbiodiniaceae and heterotrophic capacity. The calcification rate of *C. caespitosa* colonies does not change with light intensity, suggesting efficient regulation of its nutritional modes (Rodolfo-Metalpa, Huot, et al., 2008;Hoogenboom et al., 2010). *C. caespitosa* effectively manages its nutritional needs through a dynamic interplay between photosynthesis, heterotrophic feeding, calcification, and tissue composition. The coral's ability to adjust its heterotrophic feeding is as flexible as its capacity to acclimate to a variation in light conditions for photosynthesis. When both heterotrophic and photosynthetic carbon sources were limited, the corals utilized their lipid reserves to meet metabolic maintenance costs, while protein levels remained stable (Hoogenboom et al., 2010). According to this study, for colonies of *Cladocora caespitosa*, a shift in the nutritional function of heterotrophy was highlight between different light treatments. For *C. caespitosa*, enhanced feeding capacity during extended periods of darkness was associated with a reduction in photosynthetic capacity. This finding aligns with observations that corals depend more on heterotrophic carbon as depth increases, photosynthesis is limited and light availability decreases. Instead, in high light conditions, food primarily provides nitrogen and phosphorus, enabling corals to enhance tissue growth, contrasting with heterotrophy's compensatory role for carbon acquisition in the dark. Coral growth is therefore influenced by different factors: *C. caespitosa* increase its feeding capacity when acclimating to high light conditions. When light is abundant, the coral relies on heterotrophic feeding to obtain essential nutrients other than carbon (N and P). Moreover, coral colonies can increase their tissue biomass only when it has both light, which provides the energy for photosynthesis, and food, which supplies the necessary nutrients (Hoogenboom et al., 2010).

1.2.2 Asexual and sexual reproduction of *Cladocora caespitosa*

Cladocora caespitosa is characterized by a sexual and an asexual reproduction involving the formations of buds. Information on sexual reproduction is mostly available for tropical scleractinian. Few articles are centered on the reproduction of temperate corals such as *Cladocora caespitosa*. The reproductive structures are located on the mesenteries inside the

polyp and *C. caespitosa* is characterized by 24 of them per polyps. Studies had reviled one gametogenic cycle per year, oocytes and spermaries develop on separate mesenteries within each polyp. The spawning event consist in the releasing of sperm and eggs 4 days prior to the full moon in June (Kružić et al., 2008).

Regarding asexual reproduction, polyps create asexual buds by reorganizing a small area on the exosarc, which covers the distal part of the tubular corallite. Over the course of a couple of months, this area expands and develops into a functional polyp with the ability to extend tentacles. The new polyp then adjusts its growth direction in response to light stimuli, gowning parallel to the main corallite. In this period, the convex side of the corallite, opposite to the light source, grows faster than the concave side, likely by increasing the extension rate. A significantly higher rate of budding was observed in fed nubbins of *C. caespitosa* kept at high temperature, regardless of light intensity. This indicates that, under controlled experimental conditions, this coral allocates part of its energy budget to asexual reproduction, primarily during favorable conditions marked by high temperatures and increased zooplankton availability (Rodolfo-Metalpa, Peirano, et al., 2008).

1.2.3 Threats

Cladocora caespitosa is a significant species in the Mediterranean Sea, known for its ability to construct extensive reef structures. Historically, this species was able to build large reefs of kilometers long. Today, however, the population generally consist of smaller and more dispersed colonies (Kersting et al., 2023). *C. caespitosa* is increasingly threatened by general human activities in coastal zones, such as habit destruction and pollution, along with recurrent marine heatwaves in the Mediterranean Sea (Roveta et al., 2023). These heatwaves haves caused repeated mortality events, leading to an accelerated decline to this long-lived species (Roveta et al., 2023). For these reasons, the International Union for the Conservation of Nature IUCN has listed *Cladocora caespitosa* as an endangered species on the Red List (Roveta et al., 2023). According to an evaluation of the IUCN, the most extensive populations of *C. caespitosa* described to date inhabiting the Adriatic Sea, have experienced severe declines over the past decades due to a range of threats. The primary threat to this species is described to be global climate change resulting in warming seawater temperatures

and an enhancement of light irradiance and it's expected to continue and worsen in the future. Populations can recover from mortality events through the recruitment of new individuals, but the rate for this species is extremely low and insufficient to compensate the mortality rates (Casado de Amezua et al., 2015). Other threats *C. caespitosa* needs to face is the damages caused by invasive algae like *Caulerpa cylindracea* Sonder, 1845and *Lophocladia lallemandii* (Montagne, 1849) that can pose sublethal risk to recruitment and juvenile survival. Eutrophication from industrial and sewage discharges, coastal development, and historical phosphate pollution has negatively impacted some populations, particularly in the eastern Adriatic Sea and destructive activities such as trawling, dredging can also cause physical damage to coral colonies. Another important risk is represented by the high sedimentation rates from beach replenishment and dredging can lead to colony collapse, and increased water turbidity may restrict the coral's distribution depth. Overall, these combined threats contribute to the sever decline of *Cladocora caespitosa* populations (Casado de Amezua et al., 2015).

1.3 Coral's symbionts: the Symbiodiniaceae family

Unicellular algae contribute to approximately 45% of the carbon fixation on Earth. A small portion of this is accomplished by algae living in symbiosis with invertebrates, which are often found in nutrient-poor tropical waters with low plankton concentrations. In such environments, the autotrophic algae provide their invertebrate hosts with a significant competitive benefit, mainly due to the efficient recycling of nutrients between the symbiotic organisms. (Yellowlees et al., 2008). The family Symbiodiniaceae, belonging to the dinoflagellate superclass, represents the most common group of these photosynthetic endosymbionts. Their presence substantially contributes to the productivity, survival and success of their hosts as the survival of corals and other symbiotic cnidarians in the wake of environmental changes will depend on the ability of symbionts to either adapt, acclimate or both (LaJeunesse, 2002) (Goulet et al., 2005).

The Symbiodiniaceae, originally known as a single genus called *Symbiodinium*, were classified starting in the 90s when new molecular techniques identified three distinct lineages (Clade A-C). Further research using more molecular markers and wider sampling efforts uncovered six additional clades (D-I) and ongoing studies continue to find new lineages. Recent systematic revisions, which used a variety of genetic markers and considered factors like host-specificity and genome content, have redefined these clades into 15 genus-equivalent lineages (Tab. 1). These include new genera like *Symbiodinium*, formerly clade A; *Breviolum*, formerly known as clade B (LaJeunesse et al., 2018); *Philozoon*, formerly known as Temperate A (LaJeunesse et al., 2021); *Cladocopium*, formerly known as clade C and others (Nitschke et al., 2022). *Breviolum* can moreover be classified as type B1 and type B2, where B2 is common in temperate waters (Dall'Olio et al., 2022). The presence of type B2 (*Breviolum psygmophilum* (LaJeunesse, J.E.Parkinson & J.D.Reimer) J.E.Parkinson & LaJeunesse) in temperate regions of the Western Atlantic, Indo-Pacific Oceans and also Mediterranean Sea may be an indication that *Breviolum psygmophilum* is a relic from the ancient Tethys Sea. An additional possible explanation for the presence of type B2 in the Mediterranean basin is the introduction of this species during the Messinian salinity crisis (Casado-Amezúa et al., 2016).

Clade	Genus	Geographic area	Depth range	Authors
Clade A	*Symbiodinium*	Globally	Shallow-water	LaJeunesse et al., 2018
Clade B1	*Breviolum*	Greater Caribbean	Deep-water	LaJeunesse et al., 2018
Clade B2	*Breviolum*	Temperate waters	Dee-water / shallow in temperate waters	Dall'Olio et al., 2022
Temperate A	*Phylozooon*	Temperate waters	-	LaJeunesse et al., 2021
Clade C	*Cladocopium*	Indo-Pacific	Shallow and deeper waters	Nitschke et al., 2022
Clade D	*Durusdinium*	Indo-West Pacific	Shallow and deeper waters	LaJeunesse et al., 2018
Clade F	*Fugacium*	-	-	LaJeunesse et al., 2018
Clade G	*Gerakladium*	Atlantic and Pacific Oceans	-	LaJeunesse et al., 2018

Table 1 Some examples of the formerly Caldes redefined into the genus-equivalent lineages

Photosynthesis is a process through which plants and algae use light energy to transform it into glucose. This essential process involves two main stages: light-dependent reactions and light-independent reactions (Calvin cycle). The light dependent reactions take place in the thylakoid membranes of chloroplasts, where they harness light energy to produce the energy storage molecule ATP and the reduced electron carrier NADPH, which are crucial for the next stage of photosynthesis. Chlorphyll pigments play a vital role in these light-dependent reactions. Chlorophyll-a (chl-a), the primary pigment, absorbs light particularly in the blue-violet and red parts of the light spectrum. It is essential for the light-dependent reactions. In Photosystem II (large complexes of proteins and pigments optimized in harvesting light), chlorophyll-a absorbs light energy and drives the photolysis of water molecules, splitting them into oxygen, protons and electrons (Bullerjahn & Post, 1993). In addition to chl-a, certain algae like dinoflagellate contain chlorophyll-c2, an accessory pigment. Chl-c2 absorbs light in the blue-green part of the spectrum and transfers the captured energy to chlorophyll-a, thus extending the range of light wavelengths that can be utilized for photosynthesis (Larkum et al., 2020). The light-independent reactions, also known as the Calvin Benson cycle (CB cycle), occurs in the stroma of chloroplast. During this stage, carbon atoms from CO_2 are fixed and used to synthesize three-carbon sugars. This process relies on the ATP and NADPH generated during the light-dependent reactions. The Calvin Cycle is crucial for converting inorganic carbon into organic compounds, which are vital for the growth and energy needs of the organism (Larkum et al., 2020).

1.3.1 Physiological response of Symbiodiniaceae to elevated irradiance

Coral's cells symbionts can reach densities of several million or more per square centimeter of host tissue and represent one of the most abundant and important photosynthetic protist groups in tropical reef ecosystems (LaJeunesse, 2002). Symbiodiniaceae resides within the living tissue of corals, typically in the oral and aboral regions of corals. These algae are located in vacuoles (symbiosomes) within the endodermal layer of the organisms, where they experience varying light gradients from tissue surface to the skeleton. These gradients in irradiance between light-exposed and shaded tissue areas can lead to distinct distributions of the genus of Symbiodiniaceae and differential photoacclimation processes (Terán et al., 2010). *Symbiodinium* phylotypes, predominantly clades A, B and C, (now categorized as different genera, respectively *Symbiodinium*, *Breviolum* and *Cladocopium*) are typically associated with corals found at specific depth ranges (Reynolds et al., 2008). In the Caribbean Sea, Clade A *Symbiodinium* is a typically shallow-water specialists (Bongaerts et al., 2014) and the species of this lineage, cultured, are the only one known to produce measurable quantities of MAAs (mycosporine-glycine) which effectively absorbs harmful UV-B wavelengths. This capacity might offer to the host a competitive advantage under conditions of high irradiance and are rarely observed in low photic environments (Reynolds et al., 2008). Even though generally there is a predominant lineage in the host tissue, nothing excludes the possibility that there might be present, in lower concentration, different genus of *Symbiodiniaceae*: in fact, many other hosts in the same shallow-waters environments might be associated with *Breviolum*, *Cladocopium* and *Durusdinium* (LaJeunesse, 2002). If *Symbiodinium* generally is associated with shallow-water hosts, *Breviolum* (clade B) and *Cladocopium* (clade C) symbionts are generally more present in deeper water corals and are more susceptible to bleaching at elevated temperatures and high irradiance (Reynolds et al., 2008). Nonetheless, other authors suggest that *Breviolum* type B2 is indeed very common in temperate environments (even shallow waters) and can tolerate a wide range of temperature and light and can recover quickly from low temperatures (Dall'Olio et al., 2022).

Symbiodiniaceae belong to the dinoflagellates and like other algae and plants, they are characterized by pigments and photoreceptors able to capture light at different wavelength such as phytochromes, able to capture far-red and infrared light (Sorek & Levy, 2012). In situations where light levels exceed normal concentrations, excess light energy cannot be

efficiently stored photochemically, resulting in the formation of damaging free radicals that can harm the photosynthetic apparatus, specifically PSII, and the host. Research has shown that in well-pigmented corals the local light field in the cavities of the skeleton is slightly enhanced with respect to the light environment that the microalgae would see outside the structure. However, in corals that might lose Symbiodiniaceae, light will accumulate (as symbionts that absorb it are reduced) and can become higher than the external conditions leading to photoinhibition and potentially permanent damage (Terán et al., 2010). Under stressful conditions, such as high temperatures and excessive light, corals and their photosynthetic algae deploy various photoprotection mechanisms to prevent the breakdown of their symbiotic relationship (Terán et al., 2010).

An important mechanism is the non-photochemical quenching (NPQ), which dissipates safetly excess light energy absorbed by chlorophyll as heat. NPQ helps Symbiodiniaceae to manage high light conditions often encountered in shallow marine environments (Hill et al., 2005). In those conditions, the light-harvesting complexes LHCs in the chloroplasts can absorb more energy than is needed for photosynthesis leading to the formation of ROS, which can damage cellular components and contribute to coral bleaching (Hill et al., 2005). NPQ process involves the xanthophyll cycle that consist in the reversible conversion of pigments such as violaxanthin to zeaxanthin, which is a pigment that dissipate energy as heat efficiently (Hill et al., 2005). Additionally, symbionts undergo longer-term photoacclimation processes by adjusting the number and size of their phosynthetic units and the peripheral peridinin-chlorophyll-a-protein PCP antenna complexes. These adaptations help manage light energy more efficiently, reducing the risk of photodamage and maintaining the health of the coral-zooxanthellae symbiosis (Hill et al., 2005).

Important photoprotection mechanisms involves specifically *Symbiodinium*, good at performing a process called PSII-independent cyclic electron transport (CET) and chlororespiration. This means that electrons can circulate without using photosystem II and oxygen can acts as an alternative acceptor for electrons during photosynthesis. In this way, chlororespiration supports CET and helps producing ATP (indispensable for the second cycle of photosynthesis) even when PSII is unactive (Ferreira et al., 2023). Another photoprotection process is the ability to dissociate the PCP antenna complexes from PSII when *Symbiodinium* is exposed to high light. These mechanisms enable corals to effectively

manage the challenges posed by high light and temperature conditions, ensuring the maintenance of their symbiotic balance (Ferreira et al., 2023; Reynolds et al., 2008).

There can be some differences among different Symbiodiniaceae photoprotection mechanisms. Measuring the minimal fluorescence F0 (light emitted) from chlorophyll-a through the SIP method (measure chl-a fluorescence in response to a series of short irradiation pulses (SIP) of 1 second duration) both in *Symbiodinium* and *Breviolum*, it can be observed that F0 increases at first in Symbiodinium indicating a progressive saturation of the electron acceptor pool for PSII. Meanwhile, *Breviolum* seems to maintain a linear electron transport activities between PSII and PSI. This suggests a more robust electron transport system in these cells compared to *Symbiodinium* (Reynolds et al., 2008). Moreover, in *in hospite* cells, hosts with *Symbiodinium* showed a marked decrease in Fm (maximal fluorescence), but not those with *Breviolum* reflecting a strong induction of NPQ and decreased light energy transfer to PSII. Finally, it is worth to mention that when algae are illuminated with wavelengths longer than 700nm (near infrared/infrared light), there is an enhancement of fluorescence peaks that would reflect intrinsic antenna translocation from PSII to PSI (Reynolds et al., 2008).

Symbiodinium found in shallow water have kept some old mechanisms like cyclic electron transport CET, chlororespiration and the separation of antenna complexes from light-harvesting complexes. These mechanisms help them survive heat stress and damage to PSII by supporting energy production and combining with other protective mechanisms like xanthophyll de-epoxidation and UV-protective compounds. *Breviolum*, *Cladocopium* and *Durusdinium* are similar to shade plants because they are usually found in deeper water, where they need better light-harvesting abilities. The types of *Breviolum* that live in shallow water and likely use different protection methods instead of moving antenna complexes. *Breviolum* and *Cladocopium* in deeper corals, which are more prone to bleaching, can use NPQ and varying degrees of chlororespiration. However, they mainly rely on linear electron transport for photosynthesis, not CET (Reynolds et al., 2008).

Another typical response to face an excess of irradiance or high temperature is the regulation on the number and density of the symbionts in the host. Symbiodinaceae abundance generally increase in conditions of reduced light intensity with an increase also of the

photosynthetic capacities, but it also have been described the opposite where in reduced-light conditions, zooxanthellae density showed a decrease (Titlyanovl et al., 1999). Symbiodiniaceae density is influenced also by the depth of the coral: their abundance decreases as depth increases likely due to the availability of light (Widiarti et al., 2016). Nonetheless is important to remember that symbionts' density is also closely related to the different spectrum of light affecting the coral and might vary in relation to the reactions of the coral to contrast the possible damages caused by different spectrum (chapter 1.1.4).

1.3.2 Behavior of Symbiodiniaceae in Mediterranean sea's scleractinian *Cladocora caespitosa* (Linnaeus, 1767)

In Mediterranean Sea it is hard to assess the distribution of Symbiodiniaceae, due to the lack of knowledge in this area. The very few studies indicated the "Temperate A" clade (*Philozoon*), found endemic of the Mediterranean Sea and North-East Atlantic, as the dominant clade in the western basin of the Mediterranean Sea (Casado-Amezúa et al., 2014; Visram et al., 2006). *Cladocora caespitosa* (Linnaeus, 1767) sampled in different areas such as Ischia, Gulf of Triest (Italy), Cyprus and along the Israel coast was found dominated by *Symbiodinium* B2 (now assessed as *Breviolum* type B2) as indicated in Table 1.2 (Meron et al., 2012; Lajeunesse et al., 2012; Hadjioannou et al., 2019; Dall'Olio et al., 2022), while in other areas of the basin was dominated by clade temperate A *Symbiodinium* (*Philozoon*) suggesting a variation in Symbiodiniaceae association within the same host species that might be dependent on regional environmental conditions (Casado-Amezúa et al., 2014). *Breviolum* type B2 is characterized by a quickly recover in photosynthetic rates from cold temperatures meaning that they can help the host during stressful times (Casado-Amezúa et al., 2014).

Clade	Genus	Collection site	Depth	Authors
B2	*Breviolum*	Cyprus, Levantine basin	< 4 m	Hadjioannou et al., 2019
B2	*Breviolum*	Ischia island, Italy	3-7 m	Meron et al., 2012
Temperate A	*Philozoon*	Banyuls, France	-	Visram et al., 2006
B2	*Breviolum*	Israel	-	Lajeunesse et al., 2012
Temperate A B2	*Philozoon* *Breviolum*	Gulf of triest, Italy	-	Dall'Olio et al., 2022
Temperate A	*Philozoon*	Balearic Sea	-	Casado-Amezúa et al., 2014

Table 2.2 Clades of Symbiodinaceae found in C. caespitosa *collected in various sites of the Mediterraean Sea and the recent genus related*

Cladocora caespitosa occurs naturally with varying densities of symbionts within polyps of the same colony and it has been proved that as the number of zooxanthellae increases, the rate of photosynthesis increases in a non-linear way meaning that at high concentrations of zooxanthellae, each symbiont produces less carbon for the host compared to when there are fewer symbionts. On the other hand, the rate of respiration increases as the number of cells increases. This shows that more symbionts lead to higher overall respiration contributing to the total respiration of the coral colony (Hoogenboom et al., 2009). Moreover, the relationship between the number of symbionts and the amount of chlorophyll analyzed is linear, meaning that as the number of symbionts increases, the chlorophyll content increases proportionally. This indicates that the non-linear increase in the rate of photosynthesis with more symbionts is not due to changes in chlorophyll concentration. The shape of the photosynthesis rate curve is influenced by factors other than just the amount of chlorophyll. Inconsistences in those kinds of results might be explained by the different clade/genus hosted in different organisms that can affect coral growth and phosynthetic rate (Hoogenboom et al., 2009). Compared to tropical corals, *C. caespitosa* exhibit a higher density of zooxanthellae and concentration of chlorophyll in agreement to a mechanism of adaptation to shaded environment. Temperate zooxanthellae show a higher tolerance to temperature changes meaning that they are particularly resistant to elevation in temperature with no particular reduction in Fv/Fm and even exposed to 32°C they would not lose the symbionts. In particular, when exposed to 32°C, *C. caespitosa* displayed no significant reduction in the maximal photosynthetic efficiency Fv/Fm, although a decrease in the electron transport rate ETR and an increase in NPQ were observed. This indicates that the PSII of the symbionts in *C. caespitosa* was not damaged

by the elevated temperature but could not tolerate the high energy levels, resorting to NPQ to dissipate the excess energy for photoprotection. This suggest that PSII damage is a secondary effect of temperature stress, with the initial response being an increase in NPQ due to a limitation in electron flow, followed by over-reduction of the electron transport chain leading finally to a significant PSII damage. Zooxanthellae in the Mediterranean *C. caespitosa* likely have obtained some genetic adaptations to large and transient changes in temperature (Hoogenboom et al., 2009). If we look at the lineages in this study carried out by Hoogenboom et al. in 2009, *C. caespitosa* was found to host clade A *Symbiodinium* which are characterized by a particular resistance to large temperature fluctuations (Hoogenboom et al., 2009). When exposed to both light and temperature different conditions, it has been observed that with low but constant temperature such as 18°C and an increase in light intensity from 30 to 250 μmol m^{-2} s^{-1}, it was not highlighted any sort of changes in symbionts concentration or in the content of chlorophyll. It is possible that no changes were detected because the coral did not undergo photoacclimation in terms of adjusting their pigment and cell densities, especially since light was the only changing factor. Secondly, *C. caespitosa* is found in various habitats ranging from turbid to sunlit, potentially experiencing higher light levels than those simulated in this study (Rodolfo-Metalpa, Huot, et al., 2008a). *C. caespitosa* exhibit a rapid adaptation to a wide range of light levels; when exposed to high light, the coral enhances its light harvesting efficiency through the development of non-photochemical quenching mechanisms, resulting in increased maximum photosynthetic rates, saturation irradiances and respiration rates. In low light conditions, *C. caespitosa* reduces all photosynthetic parameters to maximize capture of available light. When both temperature and light conditions are altered, the coral adjust all photosynthetic components, including pigment concentration and symbiont density. At lower light intensity the photosynthetic rate is also saturated compared to electron transport rates (Rodolfo-Metalpa, Huot, et al., 2008a).

1.3 Aim of the study

Studies on the effects of different light spectrum in Scleractinian corals are focused in particular in the visible, UV and Red spectrum (Zhou et al., 2017;Wijgerde et al., 2014;Mass et al., 2010). Very few studies nominate also infrared light effects on the host and the symbiont in Scleractinian (Wijgerde et al., 2014) and no study investigating the same effects specifically on *Cladocora caespitosa*. The aim of this study is then to fill the gap and investigate the role and the effects of different spectrum, specifically full spectrum (PAR light) and full spectrum plus infrared light, on the growth, health, symbionts density and photosynthetic efficiency of *Cladocora caespitosa*. This research is particularly pertinent in the context of global warming, which poses a severe threat to marine ecosystem. The Mediterranean Sea is experiencing rising sea temperatures and increased ocean acidification, both of which negatively impact coral species like *C. caespitosa*. Additionally, according to Copernicus, the European Union's Earth Observation Program, the "ESOTC 2020 Overview" indicates that Europe experienced the lowest cloud cover on record in 2020, with a coverage of 54%, a record low since satellite data recording began in 1983. Over the past four decades, there has been a noticeable trend towards decreased cloud cover in Europe, with 2020 following this pattern and exhibiting a negative anomaly of about -3% compared to the average cloud cover of 57% during the 1991-2020 reference period. This reduction in cloud cover was particularly pronounced across central Europe, which experienced some of the largest negative anomalies of around -10% (Fig. 1.6), as well as across the land areas bordering the central and eastern Mediterranean Sea. Conversely, the main regions with higher-than-average cloud cover were found across the Iberian Peninsula (European State of the Climate 2020 | Copernicus, 2020). It could be right to think that these changes in cloud cover can significantly impact the amount of infrared irradiance reaching marine environments, thus affecting the health and growth of coral species such as *Cladocora caespitosa*. Understanding these dynamics is crucial for developing strategies to mitigate the effects of climate change on Mediterranean coral reefs. These fluctuations can alter the light environment crucial for the photosynthetic processes of corals. By understanding how *Cladocora caespitosa* responds to different light spectrums, this study aims to provide insights into optimizing conditions for coral growth and resilience useful also in a restoration perspective. It is important to know about the life history traits, ecological optima and

potential threats of a target species used in restorations practices (Roveta et al., 2023). Such knowledge is essential for developing effective conservation strategies to protect and preserve Mediterranean coral reefs in the face of ongoing climate change.

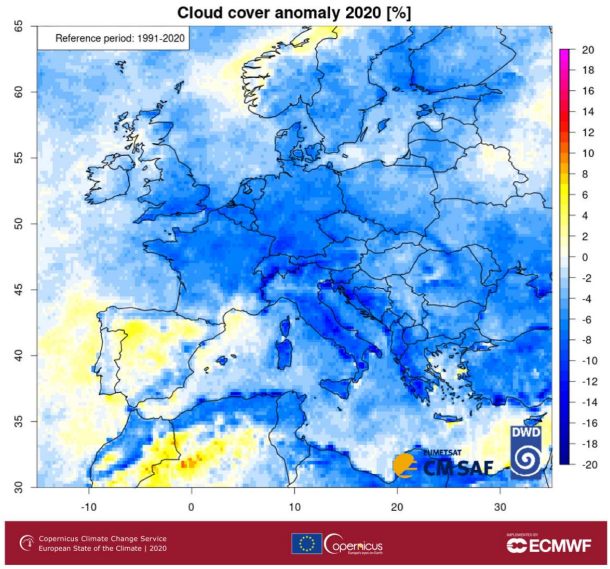

Figure 1.6 Anomalies (%) of annual mean cloud cover over the Europe region for 2020, relative to the 1991–2020 mean. Data source: CLARA-A2.1 CDR & ICDR. Credit: EUMETSAT CM SAF.

The *Objectives* of this research are the follow:

O1) Analyze the effect of different light spectra, two levels: full spectrum and full spectrum + infrared on *Cladocora caespitosa*.

O2) Simulate extreme conditions: from just two hours of infrared light per day to full day infrared illumination

The *Research questions* leading the study are:

RQ1) How *Cladocora caespitosa* reacts when exposed to infrared light?

RQ2) Will the effects be more obvious with the extreme conditions?

The three-hypothesis formulated:

H1) No differences in morphometric and morphological parameters were detected in Cladocora caespitosa exposed to infrared light *vs C. caespitosa* exposed to PAR;

H2) No alteration detected in *C. caespitosa* in its symbiont's photophysiology when exposed to infrared light *vs C. caespitosa* exposed to PAR;

H3) No alteration detected in morphometric, morphological and in symbiont's photophysiology parameters in *C. caespitosa* when exposed to 10 hours of infrared light vs when exposed to PAR.

To test our hypothesis, this study employed monthly samplings to analyze each parameter using image software analysis, stereomicroscopic observation, PAM analysis, and the extraction and determination of symbionts and chlorophyll concentration. The research hypothesized that *Cladocora caespitosa* would show no variation in morphometric and photobiological parameters, including height, area, symbiont density, and chlorophyll concentration, between the two treatments.

In the following table (table 1.2) are summarized the issue, objectives, research questions, hypothesis and methods followed of this thesis.

Issues	Objectives	Research questions	Hypothesis	N.	Methods
Coral growth and the photophysiology of its symbionts are mainly influenced by temperature and irradiance. The quality of light, characterized by its spectrum, can variably impact the growth of this coral, Symbiodinium and chlorophyll concentrazion and photosynthetic efficiency. *Cladocora caespitosa* is an endemic scelractinian of the Mediterranean Sea and the study of the photobiology of this species could allow to optimize eventual restoration actions considering the enhancement of sea temperature due to global warming.	To analyze the effects of different light spectrum, two levels (full spectrum and full spectrum+IR) and temperature, two levels (20 and 23°C) on *Cladocora caespitosa* growth (area of the colony and height), budding rate, Symbiodinium density, chlorophyll concentration and different behavior tested with a time-laps	How *Cladocora caespitosa* react when exposed infrared light? How does light can affect the coral growth and the symbionts' dynamics?	Cladocora caespitosa does not show any alterations in morphometric and morphological paremeters between the control treatment (full spectrum) and the treated colonies (full spectrum+IR)	1	Monthly sampling (T1, T2 and T3) measuring the area and the heigh trough the use of ImageJ. Budding rate through the observation at the stereomicroscope and Symbiodinium concentration through the exctraction and Neubauer counting
			Cladocora caespitosa do not show any alterations photophysiological parameters between the control treatment (full spectrum) and the treated colonies (full spectrum+IR)	2	Monthly sampling measuring Fv/Fm, Y(II), NPQ parameters with PAM and chl-a, -c concentration with the spectrofluorometer from the same corallites used for the Neubauer counting
	Simulate extreme conditions where parameters could have the greatest impact on *C. caespitosa* corals and comparison with natural simulation	Will the effects be more obvious when the colonies are exposed to infrared light for 10 hours?	No changes detected in the colonies exposed all day to full spectrum light + IR light	1	Monthly sampling (T1, T2 and T3) of colonies from the treated tanks with extreme conditions measuring the area and the heigh trough the use of ImageJ. Budding rate through the observation at the stereomicroscope and Symbiodinium concentration through the exctraction and Neubauer counting
				2	Monthly sampling from the treated tanks with extreme conditions measuring Fv/Fm, Y(II), NPQ parameters with PAM and chl-a, -c concentration with the spectrofluorometer from the same corallites used for the Neubauer counting

Table 1.2 Schematic representation of the issues, objectives, questions, hypothesis and methods and of this thesis

2. MATERIALS AND METHODS

2.1 Experimental design

The study consists in two experimental designs: one conducted from October to December 2023 and the second one from January to March 2024. For both experimental designs, eight tanks were set up within the university aquaria facility, following the illustration in Figure 2.1. After an initial acclimatization period of approximately three weeks at 18°C, the tanks were gradually divided into two groups based on temperature. Four tanks were adjusted to 20°C, while the remaining four were set to 23°C. Each temperature group consisted of two control tanks, which were illuminated by white light (FS, full spectrum) for 10 hours per day, and two experimental tanks, which were illuminated by a combination of white light and infrared light as indicated in Fig 2.1: in the first set-up experiment the infra-red light was activated two hours per day (one hour in the morning and one hour in the evening), while in the second set-up experiment the infra-red light was active for 10 hours per day, like the FS (full-spectrum) illumination.

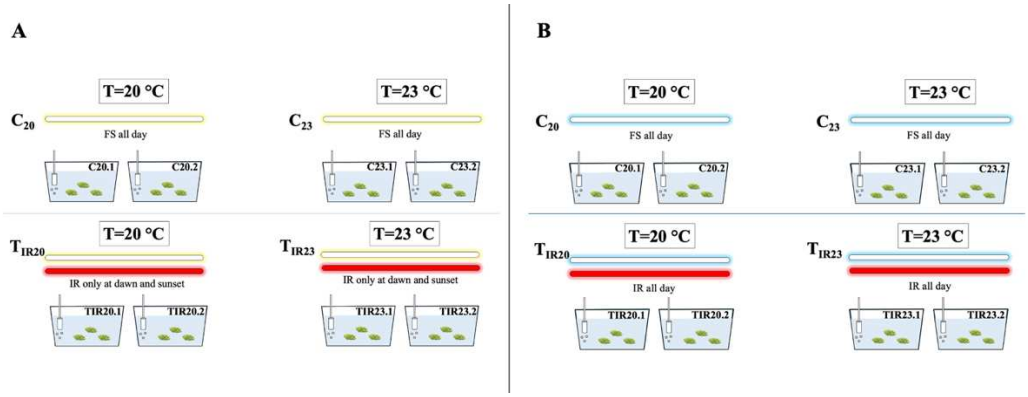

Figure 2.1 Schematic representation of the experimental design; A) October-December 2023, two hours per day of infrared; B) January-March 2024, extreme conditions simulation with IR 10 hours

In each experimental tank, three colonies of *Cladocora caespitosa* were housed and fed 1 ml of zooplankton diluted in 30 ml of water once a week. Data were collected in three periods: T1, T2, and T3, each corresponding to monthly intervals. During each sampling, data on photosynthetic and morphological parameters were recorded through the acquisition and subsequent analysis of photographs.

In the first experiment, each sample was assigned a unique ID in order to recognize each colony consisting of the tank name (C20.1, C20.2, TIR20.1, TIR20.2, C23.1, C23.3, TIR23.1 e TIR23.2) followed by the letters a, b and c to identify the three different samples within each tank (Table 2.1a). In the second experiment, a numeric ID was in this case attached to each colony and, if the number repeated itself, an alphabetical identifier was added ("a" and "b") (Table 2.1b).

A

Sample ID			
C20.1a	TIR20.1a	C23.1a	TIR23.1a
C20.1b	TIR20.1b*	C23.1b	TIR23.1b
C20.1c*	TIR20.1c	C23.1c*	TIR23.1c*
C20.2a	TIR20.2a	C23.2a	TIR23.2°*
C20.2b*	TIR20.2b	C23.2b*	TIR23.2b
C20.2c	TIR20.2c*	C23.2c	TIR23.2c

B

Sample ID			
C20.1_59*	TIR20.1_55a*	C23.1_56b*	TIR23.1_60
C20.1_51	TIR20.1_44	C23.1_42	TIR23.1_48*
C20.1_55b	TIR20.1_53b	C23.1_47	TIR23.1_61
C20.2_53a	TIR20.2_49*	C23.2_NT	TIR23.2_NTSR
C20.2_56a*	TIR20.2_54a	C23.2_40*	TIR23.2_52*
C20.2_45	TIR20.2_50	C23.2_43	TIR23.2_54b

Table 2.1 Summary of sample ID of the A) first experimental design and B) second experimental design

Samples marked with "*" indicate those from which a corallite was taken during each sampling for the extraction and counting of *Symbiodinium* in the laboratory. The morphological parameters examined included area, height, number of polyps per colony, number of buds per colony, and bleaching levels (measured using the official Reef Check color scale). Data were recorded in a customized datasheet.xls file designed for this experimental setup. In another worksheet, zooxanthellae count data were entered to calculate the concentration and the mitotic index in percentage. Zooxanthellae data were then standardized based on the dry weight of each corallite from which cells were extracted to get the standardized concentration of symbionts for each sample examined.

Due to the limited availability of expendable corallites for symbionts counts, a single corallite per tank (two corallites per treatment type) was selected, and two sub-samples were taken from each. After analysis, these samples were placed in 90% acetone and stored at 3°C until spectrophotometric analysis to determine chlorophyll-a and c_2 concentrations.

The only difference between the two experiments was the duration of exposure, while the parameters, methods, and protocols used were consistent across both experiments.

2.2 The tanks

The tanks were maintained at the university's animal facility where salinity, temperature, pH and turbidity were checked weekly. The tanks, 35 cm high, 31 cm wide and 42 cm long, contained about 40 liters of water. The illumination system consisted of two different LEDs: the Cosmorrow LED, composed by light from 500nm to 730nm, with 33% infrared light (730nm) (Fig. 2.2A) and the SilverMoon Marine LED, composed of PAR (57%) and 43% of blue light (460nm) (Fig. 2.2B) and a PAR intensity of 60. Control samples were illuminated by SilverMoon Marine LED, henceforward “PAR”, while treatment samples by both illumination systems, henceforward “PAR+IR”.

The three coral colonies were placed on top of a PVC structure at an equal height from the surface so that they all received the same amount of light from the lamp. At the beginning of the experiment, September 2023, the DIVING-PAM was used to evaluate the frequency of light striking the tanks (PAR LIGHT) for each tank, and the same value of 30 was found for each tank. After a period of acclimatization at 18°C for two weeks, the tanks were gradually raised to 20°C and 23°C and the infrared lamp was turned on for the treatment tanks, following the experimental design (Fig. 2.2.C).

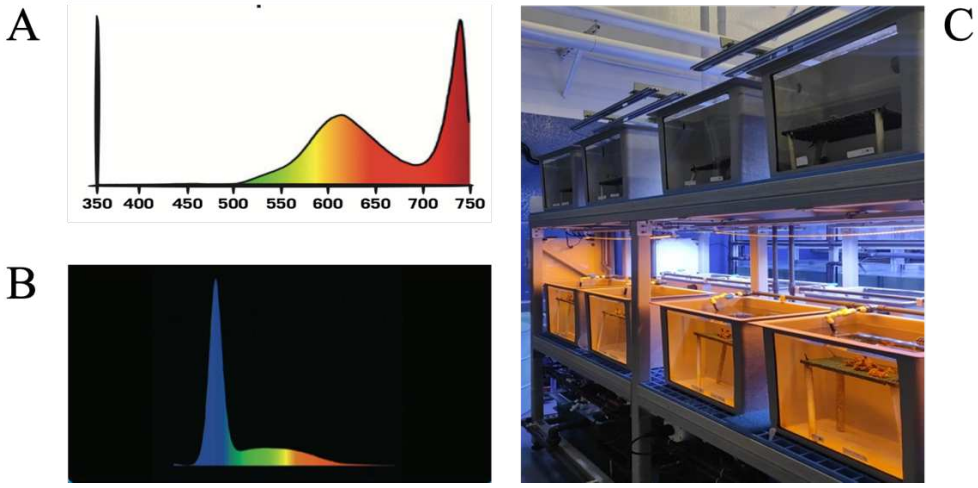

Figure 2.2 A) Light spectrum of IR LED; B) Light spectrum of PAR LED and C) Tanks illuminated with IR light (below) and PAR (above) momentarily off

2.3 Morphometric analysis

Morphometric analyses were conducted one every 20 days starting in October 2023 for the first experiment: the first ones took place on October 10, 2023 (T1), the second ones on October 30, 2023 (T2), and the third ones on November 20, 2023 (T3). The second experiment started on January 29, 2024 (T1) and the following sampling has taken place in February 29, 2024 (T2) and March 20, 2024 (T3). The parameters that were analyzed and evaluated for each sampling are: Height (cm); area (cm^2); number of buds per colony; the number of polyps in each colony and coral's condition, evaluated based on a Coral Watch colorimetric card in which a value oscillating between E1-E2 was given a value of 1; E3-E4 a value of 2; and E5-E6 a value of 3 to monitor any bleaching phenomena.

These data were collected through two methods: direct observation under a stereomicroscope (Fig 2.3a) to assess the condition and the presence and number of buds and polyps (Fig.2.3b and c) and a post-sampling analysis using ImageJ image analysis software to calculate the height and area (Fig.2.3d, e, f and g).

Figure 2.3 a) Samples under the stereomicroscope; b) C. caespitosa colony with a bud in evidence; c) C. caespitosa polyps; d&e) Area and height photos; f&g) ImageJ photo analysis

The collected data were reported in an Excel datasheet in which the percentage difference in area between T1, T2 and T3 (Δarea% cm2) and height (Δh% cm) was then calculated along with data of the number of polyps, buds and colorimetric condition of the colony later used to do statistical analysis.

2.4 Symbiodiniaceae concentration

The Symbiodiniaceae concentration was determined from a single corallite, including both soft tissues and skeleton, from each tank. The colonies from which the samples were extracted were marked with an asterisk (*) on the datasheet for identification. Each corallite was separated from its colony, placed in an Eppendorf tube, and stored in the dark at -20°C until extraction. In the laboratory, the corallite was homogenized in a mortar with a pestle, using 1 ml of artificial seawater. The homogenate was then centrifuged at 5000 rpm for 5 minutes. After centrifugation, the supernatant was removed, and the pellet was resuspended in 1 ml of artificial seawater. Zooxanthellae were counted using an Improved Neubauer hemocytometer grid (bright line BRAND Tiefe Depth Profondeur 0.01 mm 0.0025 mm^2) (Fig 2.4a) with a 10 µl volume under a Nikon C-PS N light microscope (Roveta et al., 2023). During counting, zooxanthellae (Fig 2.5) were classified into three categories: single (single rounded cells), doublets (mitotic cells with a visible cell plate and wall material between cells), and broken (cells with a visibly broken membrane). The number of doublets was recorded, and the mitotic index (%) was calculated as the ratio of doublet cells to the total number of cells per 100.

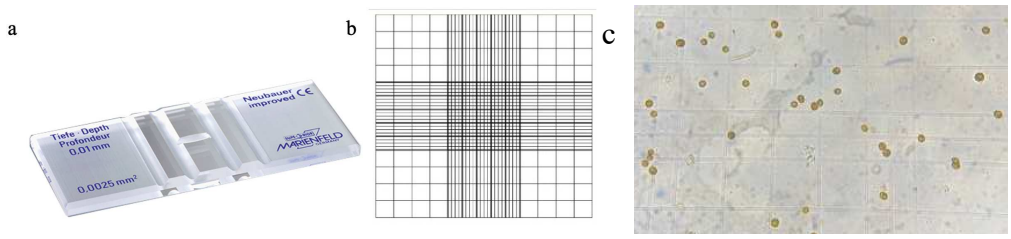

Figure 2.4 a) Improved Neubauer hemocytometer grid; b) the grid with the quadrats and c) Symbiont cells in the Neubabuer hemocytometer grid (40x)

The quadrats analyzed included the central one and the four at the corners (Fig 2.5b). Data were uploaded to the datasheet, and the average concentration was calculated and standardized based on the dry weight of the corresponding corallite. To obtain the dry weight, the corallite was placed in an oven at 60°C overnight and then weighed. Prior to this procedure, each Eppendorf tube containing the corallite and residual zooxanthellae was placed in 90% acetone for chlorophyll analysis.

2.5 Photobiology: photosynthetic efficiency, chlorophyll and photosynthetic analysis

The chlorophyll content was determined using the same corallite samples used to assess Symbiodinaceae density. Following zooxanthellae analysis, samples were preserved at -20°C in 90% acetone for chlorophyll extraction. In the Physiology of Algae and Plants laboratory of University Polytechnic of Marche, the supernatant from each sample was transferred (600 µl) into new Eppendorf tubes, which were then centrifuged for 5 minutes at 700 rpm. Samples exhibiting excessive concentration, indicated by a bright yellow coloration, were diluted and labeled accordingly. To quantify the chlorophyll concentration, a Shimadzu UV-1900i spectrophotometer was utilized. The device was calibrated with a blank sample, and each sample was subsequently placed in cuvettes for measurement. The results were then saved and analyzed.

Photobiological assessments were conducted periodically alongside morphometric evaluations. At the university's animal facility, the photosynthetic physiology of symbiotic dinoflagellate algae in corals was monitored using the pulse amplitude modulation (PAM) technique, which gauges the efficiency of Photosystem II (PSII) in photosynthesis. This technique measures the fluorescence emitted by chlorophyll in photosynthetic samples after they have been dark-adapted. Initially, the minimal fluorescence (F0) is determined using a weak light, followed by a strong light pulse to ascertain the maximal fluorescence (Fm). The difference between these two values, Fv/Fm = Fm - F0, provides the maximum quantum yield and indicates the efficiency of PSII in photosynthesis (Reynolds et al., 2008).

During sampling, the DIVING-PAM-II underwater chlorophyll fluorometer (Walz) was used. Samples were dark-adapted for 15 minutes, with measurements taken from two colonies per tank, resulting in a total of 16 samples per session, all from the same colony. The saturation kinetics of photosynthesis were described using the DIVING-PAM-II, which involved 11 steps of 20 seconds each, where the actinic light was gradually increased. Through a saturating flash, various parameters linked to photosynthetic activity were calculated: F0 (minimal fluorescence level in the dark), Fm (fluorescence after the first saturating pulse), F’m (fluorescence of saturating light flashes at intervals a), F (base

fluorescence levels after saturating flash in actinic light), Fv/Fm (maximum efficiency of PSII), Y(II) (photosynthetic efficiency of PSII), and NPQ (non-photochemical quenching).

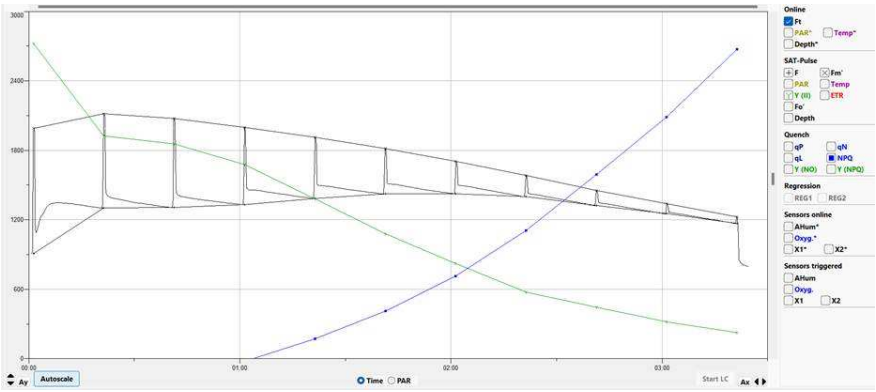

Figure 2.6 Example of a photosynthesis kinetics of C. caespitosa

2.6 Univariate analysis

To test the hypothesis that morphometric and photosynthetic parameters varied in relation to factors light (2 levels, PAR and PAR+IR), temperature (2 levels, 20°C and 23°C), and time (three levels, T1, T2 and T3), univariate analyses was performed through the 30-days free trial software PRIMER7, version 7.0.24 with PERMANOVA+. If required data were firstly square-rooted to down-weight high values across replicates within a group, in relation to those with consistently low values. The resultant data were then used to construct a Bray-Curtis similarity matrix, which was subjected to permutational multivariate analysis of variance PERMANOVA (Anderson, 2001), with the focus being on determining whether there were significant interactions between light, temperature and time. Pairwise comparisons were then performed for each significant interaction.

3 RESULTS

3.1 Morphometrics analysis

In the 2-h group, the TIR20 samples increased by 32.28% ± 15.06% SD in colony area compared to the 24.5% ± 11.73% SD of the samples from TIR23. In the 10-h experiment results are very similar to the previous ones, with TIR20 increasing by 30.2% ± 19.5% SD and TIR23 24.53% ± 22.17% SD. Overall, looking at the mean values all conditions showed a consistent, positive trend (Fig. 3.1B) with C23 in the 2-h group exhibiting the higher growth from T1 (2.59 ± 1.3 cm^2 SD) to T3 (3.03 ± 1.51 cm^2 SD). Conversely, in the 10-h group TIR23 was characterized with the higher change between T1 to T3: samples initially started with a surface area of 1.4 cm^2 ± 2 cm^2 SD and end up with a surface area of 2.8 cm^2 ± 2.7 cm^2 SD in T3 (about 50% of the initial area). Even though the results showed some differences between temperature and light treatments for both experiments, the PERMANOVA only highlighted significant differences in the area values in the 10-h experiment within the two levels of temperature (20°C and 23°C) (PERMANOVA, $p<0.05$, Tab. 3.2A), while no significance was found for the 2-h experiment (PERMANOVA, $p>0.05$, Tab. 3.1A).

About the height, in the 2-h group higher percentages were found on the C23 samples with a growth rate of about the 22.14% ± 13.5% SD and on the TIR20 samples with a value of 19.6% ± 20.06 SD [2] but no significant differences were perceived between treatments over time. In the 10-h group, results are around 10% for all samples, except for C20 with only a 5.5 ± 5.9% SD. Between the two experiments the growth rate in terms of height seems to be enhanced in the 2-h samples, so with a limited exposure to IR (Fig. 3.1C). The mean values of the growth in height showed a positive trend across all conditions and between the two different experiments, but while no significant differences were found for the 2-h experiment (PERMANOVA, $p>0.05$, Tab. 3.1B), significances were instead recorded for the 10-h experiment especially regarding light and temperature separately (PERMANOVA, $p<0.05$,

[2] The high standard deviation observed indicates a large variability among the samples taken in exams.

Tab. 3.2B), with higher values for C23 with an average height of 3.9 ± 0.9 cm2 SD in T3 and TIR23 with 2.7 ± 0.5 cm2 SD (Fig. 3.1D).

Concerning the number of buds produced in each colony, in the 2-h experiment, no consistent patter emerged along the entire period, as most colonies showed a mean value of 1 ± 2 SD bud per colony, while only for a few a small increase was registered over time (Fig 3.1E). These results were supported by the statistic in which PERMANOVA found no significant differences (PERMANOVA, $p>0.05$, Tab. 3.1C). In the second experiment, it is interesting to notice how most of the colonies started with no visible buds (except for a sample in TIR20 which was characterized by the presence of one bud) and by T3 a significant increase in the number was observed, independently from temperature and light treatment (PERMANOVA, $p<0.05$, Tab. 3.2C), especially in the C20 samples with an increment on the number of buds of around 8 ± 2.7 SD buds per colony.

A

Source	df	SS	MS	Pseudo_F	P(perm)	UP	P(MC)
Li	1	0.43221	0.43221	1.5218	0.2251	9820	0.2249
Te	1	0.00199	0.00199	0.007008	0.9336	9826	0.933
Ti	2	0.32338	0.16169	0.5693	0.5748	9955	0.561
LixTe	1	0.011316	0.011316	0.039844	0.8506	9861	0.8502
LixTi	2	0.009764	0.004882	0.017189	0.983	9942	0.9845
TexTi	2	0.003302	0.001651	0.005813	0.995	9946	0.9948
LixTexTi	2	0.00219	0.001095	0.003856	0.9959	9953	0.9956
Res	36	10.225	0.28401				
total	47	11.009					

B

Source	df	SS	MS	Pseudo_F	P(perm)	UP	P(MC)
Li	1	0.239	0.239	0.47757	0.4869	9835	0.4965
Te	1	0.99159	0.99159	1.9814	0.1696	9817	0.1684
Ti	2	0.49656	0.24828	0.49612	0.6134	9946	0.6183
LixTe	1	0.003153	0.003153	0.0063	0.9359	9820	0.9411
LixTi	2	0.008128	0.004064	0.008121	0.9908	9953	0.9926
TexTi	2	0.011141	0.005571	0.011132	0.9893	9951	0.9891
LixTexTi	2	0.053937	0.026968	0.053889	0.9506	9954	0.9465
Res	36	18.016	0.50044				
total	47	19.819					

C

Source	df	SS	MS	Pseudo_F	P(perm)	UP	P(MC)
Li	1	16.333	16.333	2.4758	0.1345	9784	0.1217
Te	1	18.75	18.75	2.8421	0.1087	9348	0.1003
Ti	2	1.125	0.5625	0.085263	0.9161	9958	0.9214
LixTe	1	0.33333	0.33333	0.050526	0.8303	9746	0.8185
LixTi	2	0.54167	0.27083	0.041053	0.9605	9959	0.9634
TexTi	2	0.125	0.0625	0.009474	0.9905	9948	0.9918
LixTexTi	2	0.54167	0.27083	0.041053	0.9623	9944	0.9606
Res	36	237.5	6.5972				
total	47	275.25					

Table 3.1 Results of three-way PERMANOVAs to test differences among light (PAR, PAR+IR), temperature (20°C and 23°C) and time (T1, T2, T3) on Cladocora caespitosa *exposed to infrared for 10h. A)Area; B) Height; C) Number of buds. Df: degree of freedoms; SS: sum of square; MS: mean square; Pseudo-F: F-ratio; P(perm): probability; UP: unique permutation; P(MC): probability with the Monte Carlo method; Li: light; Te: temperature; Ti: time.*

A

Source	df	SS	MS	Pseudo_F	P(perm)	UP	P(MC)
Li	1	0.02198	0.02198	0.1302	0.7199	9838	0.7212
Te	1	1.1568	1.1568	6.8523	**0.0137**	980	0.0138
Ti	2	0.16773	0.083863	0.49675	0.6077	9958	0.6115
LixTe	1	1.55E-05	1.55E-05	9.18E-05	0.9915	9818	0.9923
LixTi	2	0.002257	0.001128	0.006684	0.9933	9952	0.9942
TexTi	2	0.00721	0.003605	0.021355	0.9806	9952	0.9796
LixTexTi	2	0.00047	0.000235	0.001392	0.9982	9949	0.9983
Res	36	6.0776	0.16882				
total	47	7.4341					

B

Source	df	SS	MS	Pseudo_F	P(perm)	UP	P(MC)
Li	1	2.0419	2.0419	7.0185	**0.0134**	9848	0.0118
Te	1	3.9411	3.9411	13.547	**0.001**	9847	0.0009
Ti	2	0.515	0.2575	0.88509	0.4223	9946	0.4189
LixTe	1	0.3468	0.3468	1.192	0.2841	9844	0.2847
LixTi	2	0.16395	0.081974	0.28177	0.7602	9944	0.7561
TexTi	2	0.037631	0.018816	0.064675	0.9379	9955	0.9373
LixTexTi	2	0.005237	0.002618	0.009	0.99	9946	0.9907
Res	36	10.473	0.29093				
total	47	17.525					

C

Source	df	SS	MS	Pseudo_F	P(perm)	UP	P(MC)
Li	1	0.08501	0.08501	0.15274	0.7037	9830	0.5978
Te	1	0.001238	0.001238	0.002225	0.9615	9826	0.9639
Ti	2	44.761	22.381	40.211	**0.0001**	9938	0.0001
LixTe	1	0.456559	0.45659	0.82036	0.3657	9846	0.3618
LixTi	2	0.6612	0.3306	0.59399	0.5478	9956	0.553
TexTi	2	0.54332	0.27166	0.48809	0.6126	9956	0.6096
LixTexTi	2	0.62442	0.31221	0.56095	0.5818	9943	0.5784
Res	36	20.037	0.55657				
total	47	67.17					

Table 3.2 Results of three-way PERMANOVAs to test differences among light (PAR, PAR+IR), temperature (20°C and 23°C) and time (T1, T2, T3) on Cladocora caespitosa *exposed to infrared for 10h. A) Area; B) Height; C) Number of buds. Df: degree of freedoms; SS: sum of square; MS: mean square; Pseudo-F: F-ratio; P(perm): probability; UP: unique permutation; P(MC): probability with the Monte Carlo method; Li: light; Te: temperature; Ti: time.*

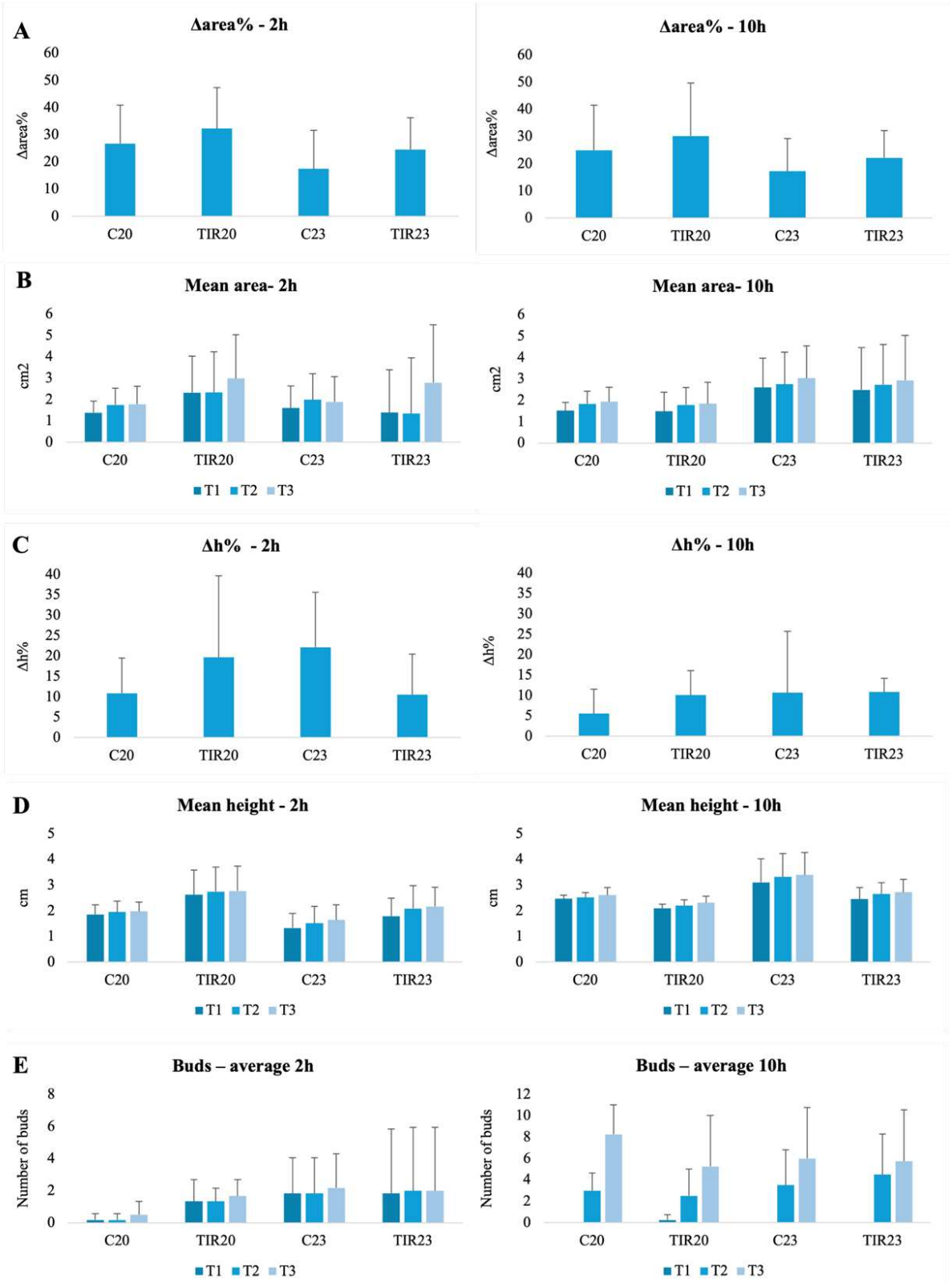

Figure 3.1 A) Difference between T3 and T1 in percentage of the area values in the first experiment "2h" and second experiment "10h"; B) Mean of the area between conditions in time; C) Difference between T3 and T1 in percentage of the height values; D) Mean of the height values in each conditions in time; E) Growth of the number of buds in time

To see if the conditions to which the corals were exposed damages the relationship between the host and the symbionts, the bleaching was monitored (Appendix, Figure 1 and 2). To do so, the Coral Watch Coral Health Chart was used to assign a value to the colorimetric state of the colony in which E1-E2 corresponds to high level of bleaching, E3-E4 medium and E5-E6 no signs of bleaching. In 2-h group we can see (Tab. 3.3, "Samples 2-h") that all the colonies except from TIR20 showed a range between E3-E4, which meant that most of the colonies showed medium or high level of bleaching. In time, it was observed that the health conditions of all the colonies decreased as the mean values attributed decreased (marked color). In 10-h group (Tab. 3.3, "Samples 10-h") the initial condition in T1 was characterized with colonies that overall did not show high levels of bleaching (except for sample C23.1_56b in which a value of E1-E2 was attributed) and in time the conditions remained constant with E3-E4 and E5-E6 for most of the samples.

Samples 2-h	T1	T2	T3	Samples 10-h	T1	T2	T3
C20.1a	E3-E4	E3-E4	E3-E4	C20.1_59	E5-E6	E5-E6	E5-E6
C20.1b	E3-E4	E1-E2	E1-E2	C20.1_51	E5-E6	E5-E6	E5-E6
C20.1c	E1-E2	E1-E2	E1-E2	C20.1_55b	E5-E6	E5-E6	E5-E6
C20.2a	E3-E4	E1-E2	E1-E2	C20.2_53a	E3-E4	E3-E4	E3-E4
C20.2b	E3-E4	E3-E4	E3-E4	C20.2_56a	E3-E4	E3-E4	E3-E4
C20.2c	E3-E4	E3-E4	E3-E4	C20.2_45	E5-E6	E3-E4	E3-E4
TIR20.1a	E5-E6	E3-E4	E3-E4	TIR20.1_55a	E3-E4	E3-E4	E3-E4
TIR20.1b	E3-E4	E3-E4	E1-E2	TIR20.1_44	E3-E4	E3-E4	E3-E4
TIR20.1c	E3-E4	E3-E4	E1-E2	TIR20.1_53b	E3-E4	E3-E4	E3-E4
TIR20.2a	E3-E4	E3-E4	E3-E4	TIR20.2_49	E5-E6	E3-E4	E3-E4
TIR20.2b	E5-E6	E5-E6	E3-E4	TIR20.2_54a	E5-E6	E5-E6	E5-E6
TIR20.2c	E5-E6	E3-E4	E3-E4	TIR20.2_50	E3-E4	E3-E4	E3-E4
C23.1a	E3-E4	E3-E4	E3-E4	C23.1_56b	E1-E2	E1-E2	E1-E2
C23.1b	E3-E4	E1-E2	E1-E2	C23.1_42	E5-E6	E5-E6	E5-E6
C23.1c	E1-E2	E1-E2	E1-E2	C23.1_47	E5-E6	E5-E6	E5-E6
C23.2a	E3-E4	E3-E4	E3-E4	C23.2_NT	E5-E6	E5-E6	E5-E6
C23.2b	E3-E4	E3-E4	E3-E4	C23.2_40	E3-E4	E3-E4	E3-E4
C23.2c	E3-E4	E3-E4	E3-E4	C23.2_43	E5-E6	E5-E6	E5-E6
TIR23.1a	E3-E4	E3-E4	E3-E4	TIR23.1_60	E3-E4	E3-E4	E3-E4
TIR23.1b	E3-E4	E3-E4	E3-E4	TIR23.1_48	E3-E4	E3-E4	E3-E4
TIR23.1c	E3-E4	E3-E4	E3-E4	TIR23.1_61	E3-E4	E1-E2	E1-E2
TIR23.2a	E1-E2	E1-E2	E1-E2	TIR23.2_NTSR	E5-E6	E5-E6	E5-E6
TIR23.2b	E3-E4	E3-E4	E3-E4	TIR23.2_52	E5-E6	E3-E4	E1-E2
TIR23.2c	E3-E4	E3-E4	E3-E4	TIR23.2_54b	E5-E6	E5-E6	E5-E6

Table 3.3 Monitoring of the bleaching in the 2-h experiment and in the 10-h experiment

3.2 Symbiodiniaceae analysis

In the 2-hours experiment, a strong decrease in Symbiodinaceae was recorded mainly considering the effect of temperature over time (PERMANOVA, $p<0.05$; Tab. 3.4A). In particular, the pairwise comparison highlighted significant differences from T1 to T2 between 20°C and 23°C sample in which those exposed to a lower temperatures showed a higher decrease ($p<0.05$; Tab. 3.4B). In fact, in the TIR20 samples with an initial concentration of 2.5 x 10^9 ± 2.7 x10^9 number of cells (n° cells) g^1 SD in T1 to 2.2 x 10^6 ± 6.0 x 10^5 n° cellg $^{-1}$ SD in T2. However, from the second sampling onward, a slightly improvement is observed. The samples exposed to 23°C showed a less critically variability from T1 to T3. In particular, the sample exposed to IR (TIR23) was characterized with a gradually reduction in the concentration of symbionts, starting with a concentration of 3.9 x 10^7 ± 3.9 x 10^6 n° cellg $^{-1}$ SD in T1 and showing in T3 a concentration of 1.6 x 10^7 ± 1.0 x 10^7 n° cellg $^{-1}$ SD. The control at 23°C (C23) showed in the last sampling an increase in their symbiont's concentrations in respect to the condition observed in T2, but a generally reduction from T1 to T3.

A

Source	df	SS	MS	Pseudo_F	P(perm)	UP	P(MC)
Li	1	1156	1156	0.88248	0.3706	9821	0.3528
Te	1	8422.1	8422.1	6.4296	**0.0124**	9843	0.0162
Ti	2	24059	12029	9.1835	**0.0003**	9944	0.0007
LixTe	1	184.31	184.31	0.1407	0.7137	9824	0.7067
LixTi	2	145.58	72.792	0.055571	0.9475	9952	0.9455
TexTi	2	29783	14891	11.368	**0.0001**	9957	0.0001
LixTexTi	2	3242	1621	1.2375	0.3188	9960	0.2931
Res	36	47156	1309.9				
total	47	1.14E+05					

B

T1

	t	P(perm)	UP	P(MC)
20,23	3.1523	**0.0102**	9780	0.0064

T2

	t	P(perm)	UP	P(MC)
20,23	6.1305	**0.0003**	9829	0.001

T3

	t	P(perm)	UP	P(MC)
20,23	0.51588	0.6053	9816	0.6198

Table 3.4 A) Results of the three-way PERMANOVA to test differences in the living symbiont concentration (2-h) among light (PAR, PAR+IR), temperature (20°C and 23°C) and time (T1, T2, T3). B) Results of posteriori pairwise comparisons within time T1, T2 and T3 depending on 20°C and 23°C. Df: degree of freedoms; SS: sum of square; MS: mean square; Pseudo-F: F-ratio; P(perm): probability; UP: unique permutation; P(MC): probability with the Monte Carlo method; Li: light; Te: temperature; Ti: time.

In the 10-hour IR exposure experiment, registered an overall strong decrease over time (PERMANOVA, $p<0.05$; Tab. 3.5A), with both T3 and T2 significantly differing from T1 (pairwise comparison, $p<0.05$; Tab. 3.5B). In T1 samples are characterized with an average of $2.8 \times 10^7 \pm 1.5 \times 10^7$ n° cellg $^{-1}$ SD, in T2 the range was about $3.9 \times 10^6 \pm 2.3 \times 10^6$ n° cellg $^{-1}$ SD while in T3 the concentration was around $4.5 \times 10^6 \pm 1.1 \times 10^6$ n° cellg $^{-1}$ SD. Temperature and light are also two factors synergically affecting the total zooxanthellae abundance (PERMANOVA, $p<0.05$; Tab. 3.5A). At 23°C, C23 displayed lower concentrations ($2.04 \times 10^6 \pm 8.9 \times 10^5$ n° cellg $^{-1}$ SD) compared to TIR23 ($7.0 \times 10^6 \pm 3.2 \times 10^6$ n° cellg $^{-1}$ SD), while under controlled conditions of light intensity C20 had lower concentrations ($1.8 \times 10^6 \pm 9.8 \times 10^5$ n° cellsg $^{-1}$ SD) compared to TIR20 ($4.9 \times 10^6 \pm 4.3 \times 10^6$ n° cellsg $^{-1}$ SD) (pairwise comparison, $p<0.05$; Tab. 3.5B).

A

Source	df	SS	MS	Pseudo_F	P(perm)	UP	P(MC)
Li	1	511.23	511.23	9.7922	**0.0035**	9838	0.0037
Te	1	0.44603	0.44603	0.0085433	0.9231	9834	0.9287
Ti	2	7598.7	3799.4	72.774	**0.0001**	9952	0.0001
LixTe	1	380.45	380.45	7.2873	**0.01**	9821	0.0097
LixTi	2	192.31	96.157	1.8418	0.1749	9940	0.1715
TexTi	2	189.27	94.635	1.8127	0.1734	9963	0.1745
LixTexTi	2	256.23	128.11	2.4539	0.097	9956	0.1028
Res	36	1879.5	52.208				
total	47	11008					

B

20°C

	t	P(perm)	UP	P(MC)
PAR, PAR+IR	0.28942	0.7713	9833	0.7767

23°C

	t	P(perm)	UP	P(MC)
PAR, PAR+IR	4.3502	**0.0003**	9851	0.0006

Ti

	t	P(perm)	UP	P(MC)
T1, T2	9.3747	**0.0001**	9820	0.0001
T1, T3	10.217	**0.0001**	9841	0.0001
T2, T3	1.8649	0.0739	9846	0.0716

PAR

	t	P(perm)	UP	P(MC)
20,23	2.2737	**0.0382**	9834	0.0378

PAR+IR

	t	P(perm)	UP	P(MC)
20,23	1.7038	0.1049	9839	0.1098

Table 3.5 A) Results of the three-way PERMANOVA to test differences in the living symbiont concentration (10-h) between light (PAR, PAR+IR), temperature (20°C and 23°C) and time (T1, T2, T3); B) Results of posteriori pairwise comparisons within temperature (20°C and 23°C) depending on PAR and PAR+IR, within light (PAR and PAR+IR), depending on temperature (20°C and 23°C) and time Ti. Df: degree of freedoms; SS: sum of square; MS: mean square; Pseudo-F: F-ratio; P(perm): probability; UP: unique permutation; P(MC): probability with the Monte Carlo method; Li: light; Te: temperature; Ti: time.

The results of the 2-h experiment showed significant differences between light treatments in the MI (PERMANOVA, $p<0.05$, Tab 3.6), with lower values in the TIR treatment (11%) compared to the control (6%). On the other hand, the results from the 10h-experiments suggest a significant change in the MI over time (PERMANOVA, $p<0.05$, Tab 3.7), with a decreasing trend from T1 (15%) to the following time steps (T2 with 11% and T3 with 7%).

In particular, in C20 a decrease of 22.07% of the MI was recorded, specifically from 28.22% in T1 to 6.15% in T3, while in TIR23 a decrease of 7.53% from T1 to T3 was observed (Fig. 3.2B).

Source	df	SS	MS	Pseudo_F	P(perm)	UP	P(MC)
Li	1	28.485	28.485	4.7698	**0.0317**	9806	0.0375
Te	1	0.10779	0.10779	0.01805	0.8996	9858	0.8945
Ti	2	23.05	11.525	1.9299	0.1624	9958	0.1624
LixTe	1	0.10193	0.10193	0.017068	0.8991	9844	0.8952
LixTi	2	10.142	5.0712	0.84918	0.4393	9941	0.4378
TexTi	2	7.3161	3.658	0.61254	0.5447	9954	0.5437
LixTexTi	2	4.4321	2.2161	0.37108	0.6814	9947	0.6898
Res	36	214.99	5.9719				
total	47	288.62					

Table 3.6 Results of the three-way PERMANOVA to test differences in mitotic index MI (2-h)between light (PAR, PAR+IR), temperature (20°C and 23°C) and time (T1, T2, T3). Df: degree of freedoms; SS: sum of square; MS: mean square; Pseudo-F: F-ratio; P(perm): probability; UP: unique permutation; P(MC): probability with the Monte Carlo method

Source	df	SS	MS	Pseudo_F	P(perm)	UP	P(MC)
Li	1	0.08802	0.08802	0.13577	0.728	9850	0.7197
Te	1	0.46952	0.46952	0.72424	0.405	9831	0.4025
Ti	2	6.4308	3.2154	4.9598	**0.0114**	9963	0.0138
LixTe	1	2.4576	2.4576	3.7909	0.0546	9825	0.0585
LixTi	2	0.89481	0.4474	0.69012	0.5227	9951	0.5062
TexTi	2	0.37695	0.18847	0.29072	0.7555	9957	0.7542
LixTexTi	2	1.5937	0.79683	1.2291	0.3039	9951	0.3071
Res	36	23.339	0.6483				
total	47	35.65					

Table 3.7 A) Results of the three-way PERMANOVA to test differences in mitotic index MI (10-h)between light (PAR, PAR+IR), temperature (20°C and 23°C) and time (T1, T2, T3). Df: degree of freedoms; SS: sum of square; MS: mean square; Pseudo-F: F-ratio; P(perm): probability; UP: unique permutation; P(MC): probability with the Monte Carlo method

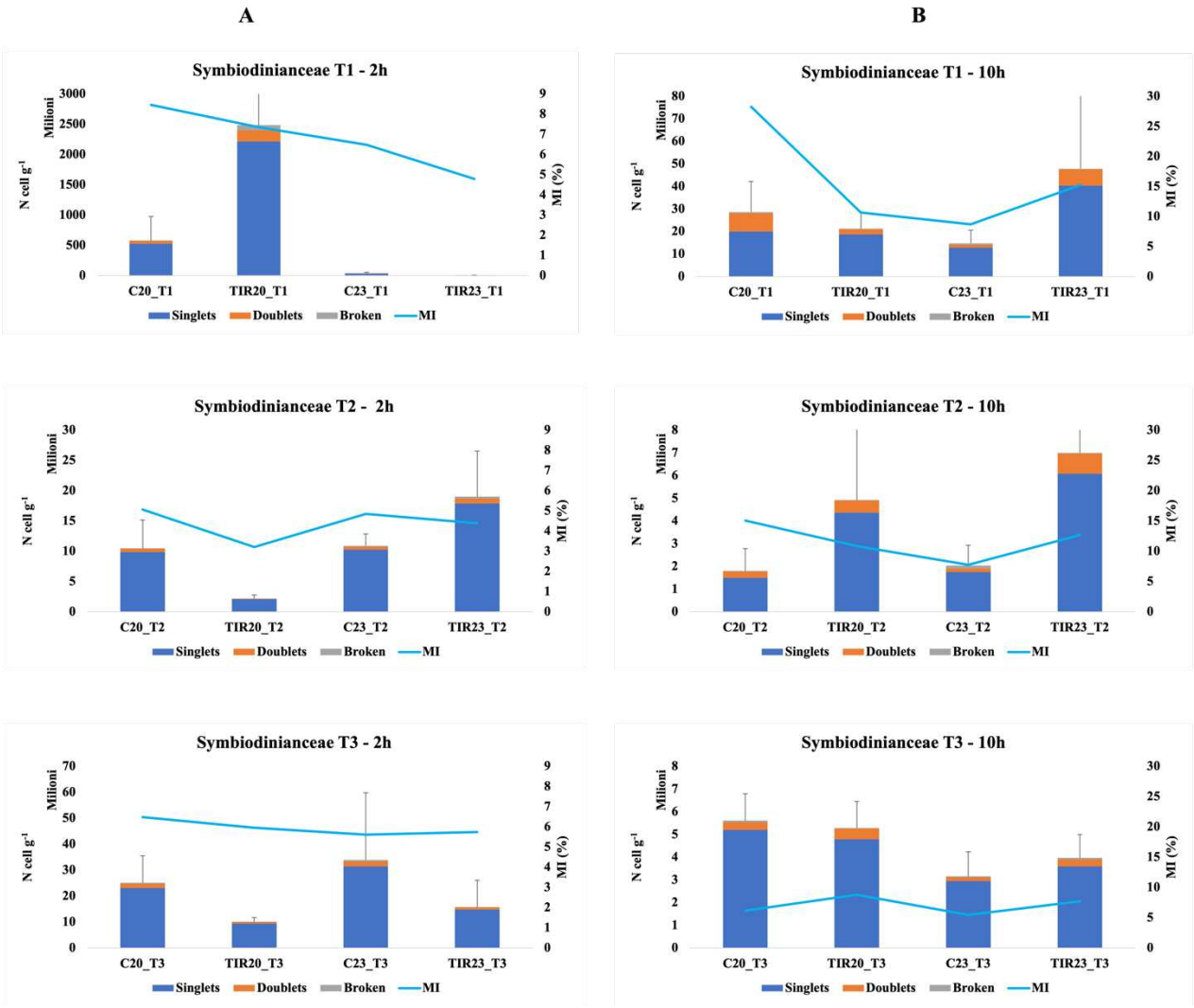

Figure 3.2 A) 2-h group trend of Symbiodiniaceae concentration; B) 10-h group trend of Symbiodiniaceae concentration

During the evaluation of symbiont concentration within *C. caespitosa*, the quality of the cells was also assessed (Fig. 3.3), categorizing them into three main groups: singlets, doublets and broken cells. The results show that in both experiments most cells found are singlets (Fig. 3.3A&B).

In the 2-h experiment (Fig. 3.3A), the percentage of doublets found was lower than the previous results. In particular, considering all treatments, the higher value observed was in C20 with $4.9 \times 10^7 \pm 3.9 \times 10^7$ n° cellg $^{-1}$ of doublets in T1; this value then decreased until in T3 reaching $2.5 \times 10^7 \pm 1.1 \times 10^6$ n° cellg $^{-1}$. Overall, the PERMANOVA revealed a complex scenario with the number of broken cells varying in time depending on the light and

temperature treatment ($p<0.05$, Tab 3.8A). The pairwise test revealed a significant decrease over time in both control samples C20 and C23, while the infrared influenced significatively the decrease over time in 20°C samples ($p<0.05$, Tab. 3.8B).

A

Source	df	SS	MS	Pseudo_F	P(perm)	UP	P(MC)
Li	1	47.071	47.071	0.20005	0.6675	9847	0.6609
Te	1	928.9	928.9	3.9478	0.0532	9830	0.0537
Ti	2	7276.2	3638.1	15.462	**0.0001**	9961	0.0001
LixTe	1	375.74	375.74	1.5969	0.2259	9859	0.2129
LixTi	2	670.27	335.14	1.4243	0.23	9946	0.2492
TexTi	2	2760.3	1380.2	5.8656	**0.0021**	9949	0.0069
LixTexTi	2	1802.4	901.18	3.83	**0.021**	9949	0.0333
Res	36	8470.7	235.3				
total	47	22332					

B

PAR

	t	P(perm)	UP	P(MC)
20: T1vsT2	4.6018	**0.0245**	25	0.0029
20: T1VsT3	3.3242	**0.0275**	35	0.0152
20: T2vsT3	4.0067	**0.0263**	25	0.0074
23: T1vsT2	4.8653	**0.0309**	35	0.003
23: T1VsT3	4.7589	**0.0266**	35	0.0023
23: T2vsT3	2.7199	**0.028**	35	0.0352

PAR+IR

	t	P(perm)	UP	P(MC)
20: T1VsT2	2.4753	**0.0295**	35	0.0501
20: T1vsT3	2.3182	**0.0278**	35	0.06
23: T2vsT3	2.8204	**0.0274**	35	0.0289

Table 3.8 A) Results of PERMANOVA to test differences in the concentration of broken Symbiodiniaceae (2-h) between light (PAR, PAR+IR), temperature (20°C and 23°C) and time (T1, T2, T3). B) Results of posteriori pairwise three way comparisons. Df: degree of freedoms; SS: sum of square; MS: mean square; Pseudo-F: F-ratio; P(perm): probability; UP: unique permutation; P(MC): probability with the Monte Carlo method.

In 10-h experiment, the doublets experienced a decrease from T1 to T3. C20 was initially characterized by the presence of $8.1 \times 10^6 \pm 9.4 \times 10^6$ n° cellg $^{-1}$ of doublets and it decreased until reaching in T3 a value of $7.2 \times 10^4 \pm 1.2 \times 10^5$ n° cellg $^{-1}$ of doublets. Regarding the presence of broken cells, for all the conditions it was no reported high amount of it among samples. The maximum valued reached was found in C23 in T1 with a value of $6.7 \times 10^5 \pm 5.8 \times 10^5$ n° cellg $^{-1}$. The analysis of broken symbionts suggests a significant interaction across time and light (PERMANOVA, $p<0.05$, Tab. 3.9A), with C samples always showing higher values ($2.5 \times 10^5 \pm 2.3 \times 10^5$ n° cellg $^{-1}$) pairwise test, $p<0.05$; Tab. 3.9B) and with highly variable results depending on the time step considered (Fig. 3.3B).

A

Source	df	SS	MS	Pseudo_F	P(perm)	UP	P(MC)
Li	1	2.65E+05	2.65E+05	12.725	**0.0009**	9807	0.0008
Te	1	41815	41815	2.0096	0.1586	9833	0.1657
Ti	2	1.73E+06	8.67E+05	41.675	**0.0001**	9950	0.0001
LixTe	1	14.664	14.664	7.05E-04	0.9771	9819	0.9791
LixTi	2	1.53E+05	76681	3.6853	**0.0369**	9962	0.0372
TexTi	2	23076	11538	0.55451	0.582	9947	0.5776
LixTexTi	2	3.42E+04	17114	0.8225	0.445	9945	0.4531
Res	36	7.49E+05	20807				
total	47	3.00E+06					

B

T1

	t	P(perm)	UP	P(MC)
PAR, PAR+IR	2.5994	**0.0281**	9765	0.0221

T2

	t	P(perm)	UP	P(MC)
PAR, PAR+IR	3.0798	**0.0116**	9748	0.0084

Table 3.9 A) Results of the three-way PERMANOVA to test differences in the concentration of broken Symbiodiniaceae (10-h) between light (PAR, PAR+IR), temperature (20°C and 23°C) and time (T1, T2, T3). B) Results of posteriori pairwise comparisons within time T1 and T2 depending on PAR and PAR+IR. Df: degree of freedoms; SS: sum of square; MS: mean square; Pseudo-F: F-ratio; P(perm): probability; UP: unique permutation; P(MC): probability with the Monte Carlo method.

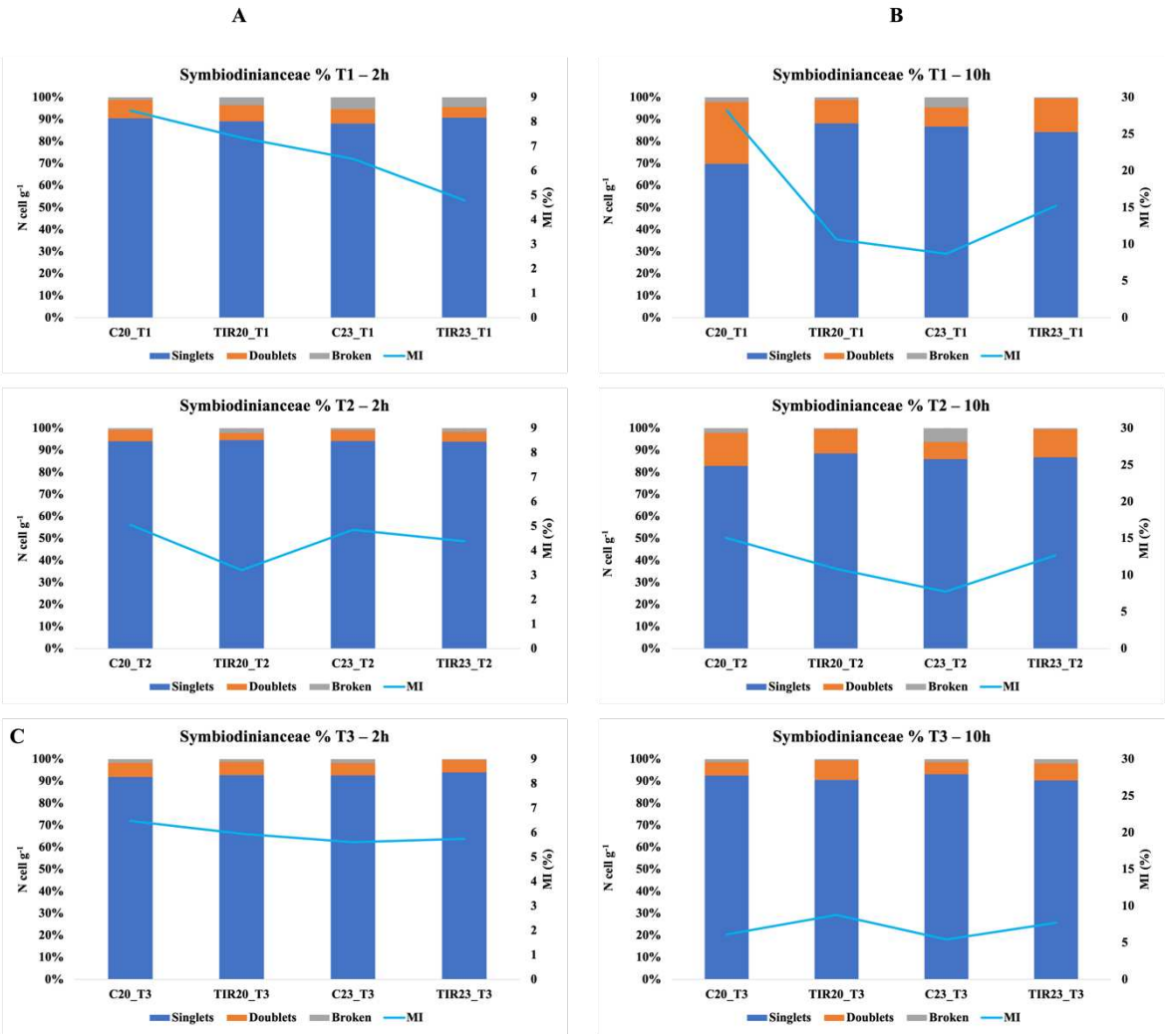

Figure 3.3 A) 2-h symbiont distribution in percentage in time; B)10-h symbiont distribution in percentage in time

3.3 Photosynthetic analyses

To assess the photosynthetic capacity and changes in the photosynthetic apparatus of the algal symbionts, chl content was measured. The chlorophyll concentration of the samples is shown in the figure 3.4. In both experiments, the concentration of chlorophyll-a was found higher than chlorophyll-c_2 (Fig. 3.4A&B). In 2-h group, no significant results were found for both the content of chlorophyll-a and chlorophyll-c_2 (PERMANOVA, $p>0.05$; Tab. 3.10). However, TIR23 at T1 had the highest levels of chlorophyll-a (9.7 ± 12.8 pg/g) following a great decrease in T3 reaching a chlorophyll-a content of 0.25 ± 0.22 pg/g. The rest of the samples was characterized by a low concentration of both chlorophyll types with a slightly decreasing trend during the entire experiment.

In the 10-h experiment, a peculiar trend was observed, with chlorophyll-a contents increasing significantly during the first half of the experiment and then decreasing significantly during the second half (Fig. 3.4). This behavior seemed to be mainly related to the light to which samples were exposed (PERMANOVA, $p<0.05$, Tab. 3.11A). In fact, the pairwise comparison showed significant differences in the 20°C treatment from T1 to T3 in which TIR20 retained more chlorophyll-a than C20 (0.8 ± 0.01 pg/g in C20 compared to 0.8 ± 0.1 pg/g in TIR20). While at 23°C revealed a significant relation between T1-T2 with C23 samples characterized by higher Chl content compared to TIR23 (1.03 ± 0.5 pg/g) and T2-T3 with 1.8 ± 0.6 pg/g of chlorophyll-a in C23 ($p<0.05$, Tab. 3.9B). Even though not supported by the statistics, a general decrease over time was observed in all treatments, samples exposed to the higher temperature (C23 and TIR23) retained a higher Chl-a concentration at T3 (1.6 ± 0.7 pg/g in TIR23 and 1.8 ± 0.6 pg/g in C23) compared to what was found in samples exposed to 20°C (0.8 ± 0.01 pg/g in C20 and 0.8 ± 0.1 pg/g in TIR20). For chlorophyll-c_2, a similar trend to the one of chl-a was found, with a first increase in the chl-c_2 from T1 to T2 and then an important decrease from T2 to T3. In this case, the PERMANOVA revealed that these differences over time were mainly related to the temperature ($p<0.05$, Tab. 3.12), as also pointed out by the pairwise comparison ($p<0.05$, Tab. 3.12B).

In order to better appreciate the results and to evaluate changes in the organization of the photosynthetic apparatus, in figure 3.4C are showed the ration between chlorophyll a and c_2. In 2-h experiment there is a clear pattern across the different sampling times characterized with an overall decrease on the ration, with T1 showing values from 3.29 ± 0.31 in TIR23 to 5.93 ±10.10 in C20, while at T3, the range narrows to 1.07 ±0.14 in C20 to 1.96 ± 0.09 in TIR23. Temporal variability was less pronounced in the results of the 10-h experiment and across the different conditions, with an overall increase in the ration in T2 for all the conditions, especially for the samples exposed to IR. In the sample exposed to IR at 20°C was observed initially a ratio of 2.61 ± 0.09 that increased in T2 up to 3.65 ±0.18, while the samples exposed to IR at 23°C exhibit an initial ration of 2.70 ± 0.27 that increase in T2 reaching a ration of 3.88 ±0.17 (Fig. 3.4C). Nonetheless these values decrease once again in T3 in which we have similar values of the initial condition.

We then evaluated the in-vivo photosynthetic activity of the symbiont. Fv/Fm results indicate the maximum photosynthetic efficiency with a general increasing trend over time for samples at 20°C, while at 23°C, control sample maintained the same value from T1 (0.62 ± 0.014) to T3 (0.62 ± 0.02), with a slightly decrease in T2 (0.59 ± 0.05). Conversely TIR23 was characterized with an overall decrease overtime, starting at T1 with a Fv/Fm of 0.63 ± 0.02, T2 with 0.61 ± 0.01 and ending up at T3 with a value of 0.58 ± 0.07 (Fig. 3.4D). The PERMANOVA did not find significant difference in 2-hours experiment, while in the 10-hours experiment the variability over time independently from the treatment was identified ($p<0.05$, Tab. 3.13). In 10-h the ratio increased overtime for all the samples with the major increase observed for C20 (from 0.39 ± 0.03 in T1 to 0.55 ± 0.01 in T3) and TIR23 (from 0.49 ± 0.08 in T1 and 0.61 ± 0.02 in T3) (Fig. 3.4D).

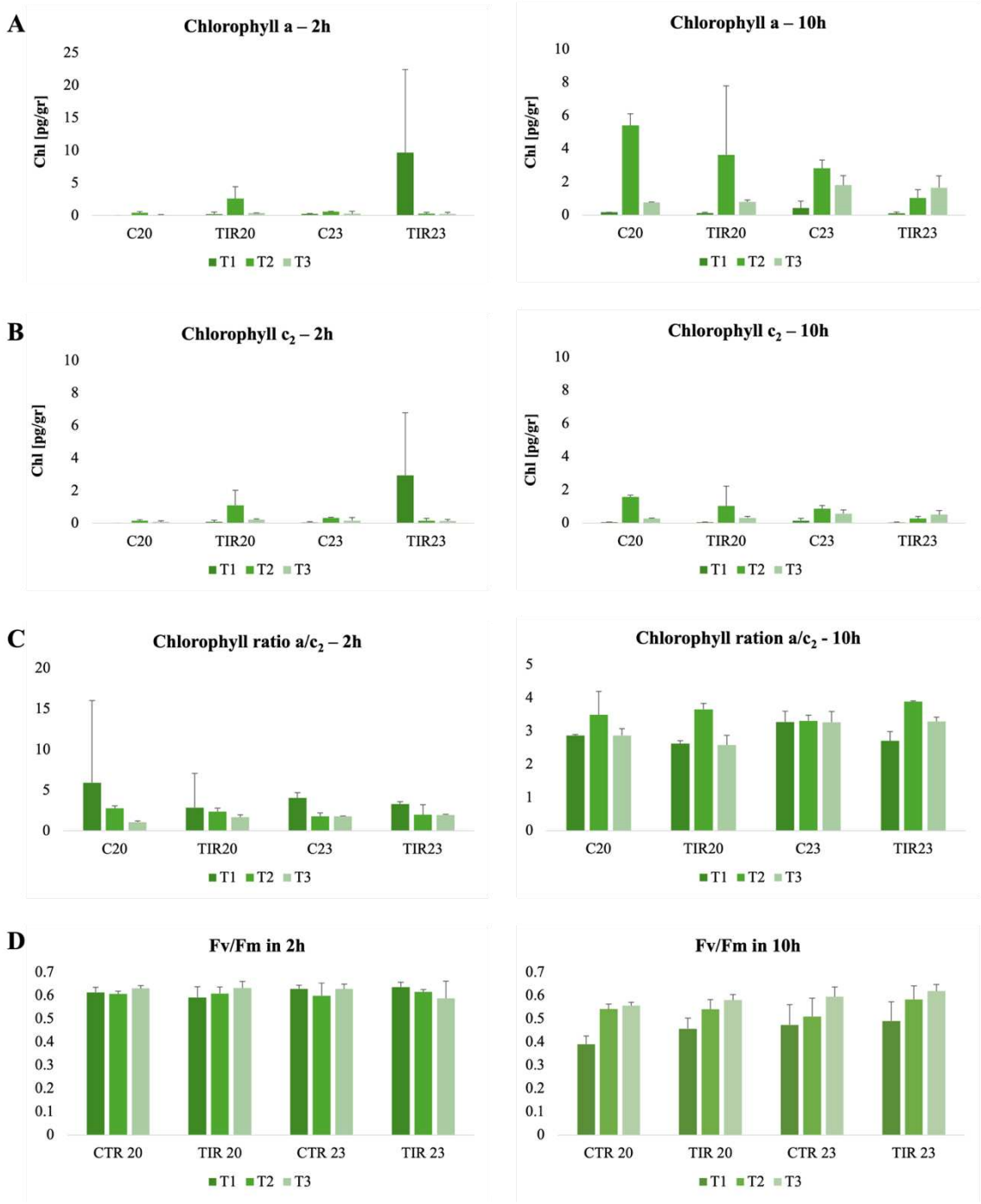

Figure 3.4 A) Chlorophyll-a concentration in the first and second experiment; B) Chlorophyll-c_2 concentrations in the first and second experiment; C) Chlorophyll ration in the first and second experiment; D) Fv/Fm values in the first and second experiment

A

Source	df	SS	MS	Pseudo_F	P(perm)	UP	P(MC)
Li	1	23.208	23.208	1.6655	0.2674	9724	0.2281
Te	1	9.6006	9.6006	0.68901	0.5018	9550	0.4209
Ti	2	21.752	10.876	0.78053	0.5948	9953	0.4839
LixTe	1	6.8739	6.8739	0.49332	0.5207	9607	0.4983
LixTi	2	25.154	12.577	0.90262	0.4969	9960	0.4362
TexTi	2	39.431	19.716	1.4149	0.2883	9957	0.277
LixTexTi	2	38.861	19.43	1.3945	0.2927	9945	0.2853
Res	36	167.21	13.934				
total	47	332.09					

B

Source	df	SS	MS	Pseudo_F	P(perm)	UP	P(MC)
Li	1	2.4622	2.4622	1.8734	0.2159	9747	0.1949
Te	1	0.74819	0.74819	0.56927	0.5146	9733	0.4633
Ti	2	1.5466	0.77332	0.58839	0.6434	9929	0.5714
LixTe	1	0.37644	0.37644	0.28641	0.5578	9730	0.5975
LixTi	2	2.2222	1.1111	0.84538	0.5192	9955	0.4541
TexTi	2	3.817	1.9085	1.4521	0.2796	9954	0.2681
LixTexTi	2	4.2336	2.1168	1.6106	0.2426	9959	0.2439
Res	12	15.772	1.3143				
total	23	31.178					

Table 3.10 A) Results of the three-way PERMANOVA to test differences in the concentration of Chlorophyll-a (A) and chl-c_2 (B) content in 2-h between light (PAR, PAR+IR), temperature (20°C and 23°C) and time (T1, T2, T3). Df: degree of freedoms; SS: sum of square; MS: mean square; Pseudo-F: F-ratio; P(perm): probability; UP: unique permutation; P(MC): probability with the Monte Carlo method.

A

Source	df	SS	MS	Pseudo_F	P(perm)	UP	P(MC)
Li	1	2.65E+05	2.65E+05	12.725	**0.0009**	9807	0.0008
Te	1	41815	41815	2.0096	0.1586	9833	0.1657
Ti	2	1.73E+06	8.67E+05	41.675	**0.0001**	9950	0.0001
LixTe	1	14.664	14.664	7.05E-04	0.9771	9819	0.9791
LixTi	2	1.53E+05	76681	3.6853	**0.0369**	9962	0.0372
TexTi	2	23076	11538	0.55451	0.582	9947	0.5776
LixTexTi	2	3.42E+04	17114	0.8225	0.445	9945	0.4531
Res	36	7.49E+05	20807				
total	47	3.00E+06					

B

T1

	t	P(perm)	UP	P(MC)
PAR, PAR+IR	2.5994	**0.0281**	9765	0.0221

T2

	t	P(perm)	UP	P(MC)
PAR, PAR+IR	3.0798	**0.0116**	9748	0.0084

Table 3.11 A) Results of the three-way PERMANOVA to test differences in the concentration of Chlorophyll-a content in 10-h between light (PAR, PAR+IR), temperature (20°C and 23°C) and time (T1, T2, T3). B) Results of posteriori pairwise comparisons within time T1 and T2 depending on PAR and PAR+IR. Df: degree of freedoms; SS: sum of square; MS: mean square; Pseudo-F: F-ratio; P(perm): probability; UP: unique permutation; P(MC): probability with the Monte Carlo method.

A

Source	df	SS	MS	Pseudo_F	P(perm)	UP	P(MC)
Li	1	0.26483	0.26483	1.9596	0.1906	9855	0.1855
Te	1	0.13701	0.13701	1.0138	0.378	9821	0.3368
Ti	2	2.9862	1.4931	11.048	**0.0011**	9958	0.0032
LixTe	1	0.010249	0.010249	0.075835	0.7367	9750	0.7863
LixTi	2	0.37999	0.18999	1.4058	0.2941	9964	0.286
TexTi	2	1.0529	0.52643	3.8952	**0.0366**	9949	0.0491
LixTexTi	2	0.000575	0.0002875	0.0021273	0.9969	9952	0.9977
Res	12	1.6218	0.13515				
total	23	6.4535					

B

20°C

	t	P(perm)	UP	P(MC)
t1,t2	2.9335	**0.0303**	253	0.045
t1,t3	7.8715	**0.0283**	270	0.001
t2,t3	2.365	0.1072	270	0.0795

23°C

	t	P(perm)	UP	P(MC)
t1,t2	4.9232	**0.0313**	270	0.0073
t1,t3	3.5237	0.0577	270	0.0251
t2,t3	0.19202	0.7491	263	0.8548

Table 3.12 A) Results of the three-way PERMANOVA to test differences in the concentration of Chlorophyll-c_2 content in 10-h between light (PAR, PAR+IR), temperature (20°C and 23°C) and time (T1, T2, T3). B) Results of posteriori pairwise comparisons within time temperature 20°C and 23°C depending on T1, T2 and T1, T3. Df: degree of freedoms; SS: sum of square; MS: mean square; Pseudo-F: F-ratio; P(perm): probability; UP: unique permutation; P(MC): probability with the Monte Carlo method.

Source	df	SS	MS	Pseudo_F	P(perm)	UP	P(MC)
Li	1	0.012417	0.012417	3.7279	0.064	9850	0.0594
Te	1	0.007675	0.007675	2.3043	0.1453	9823	0.1367
Ti	2	0.14212	0.071058	21.334	**0.0001**	9946	0.0001
LixTe	1	0.001294	0.001294	0.38852	0.5388	9833	0.5427
LixTi	2	0.002658	0.001329	0.39893	0.674	9955	0.6657
TexTi	2	0.0049	0.00245	0.73561	0.4888	9960	0.482
LixTexTi	2	0.006436	0.003218	0.96612	0.3902	9951	0.3883
Res	35	0.11658	0.003331				
total	46	0.29484					

Table 3.13 A) Results of the three-way PERMANOVA to test differences in the Fv/Fm in the 10-h experiment between light (PAR, PAR+IR), temperature (20°C and 23°C) and time (T1, T2, T3). Df: degree of freedoms; SS: sum of square; MS: mean square; Pseudo-F: F-ratio; P(perm): probability; UP: unique permutation; P(MC): probability with the Monte Carlo method

Photosynthetic efficiency of photosystem II was measured as Y(II) (Fig. 3.5), which generally decreases as light intensity increase. Depending on the conditions to which the symbiotic algae or their host are exposed to, the pattern may differ, showing a steeper or more gradual decline from the exposure to increasing light intensities. For both experiments, there is an overall reduction of Y(II) in function of the increasing of light intensity with no differences among samples. Nonetheless, we can notice that in samples of 10-h experiments (Fig. 3.5B), the initial point tends to increase in function of time. In C20, for example, the initial value, at 0 μmol $m^{-2}s^{-1}$, was 0.38 ± 0.05 and at T3 increased up to 0.55 (± 0.01). The same pattern was not observed in the 2-h experiment where all the samples were characterized by the same initial value at 0 μmol $m^{-2}s^{-1}$ in all the sampling time (Fig. 3.5A).

Regarding the NPQ values, in the results showed in figure 3.6, a clearer pattern is presented in the samples of 10-h experiment where an overall increase with the increasing of light intensity (PAR) was observed. In time, they seem to dissipate more energy, especially TIR20 where, at 1483 μmol $m^{-2}s^{-1}$ in T1 the NPQ was around 0.79 (± 0.11) and increased up to 3.01 (± 0.36) in T3 (TIR20) and in TIR23, where it was initially characterized by an NPQ of about 0.69 (± 0.22) at 1483 μmol $m^{-2}s^{-1}$ and reached in T3 a value of 2.32 (± 0.78) (Fig. 3.6B).

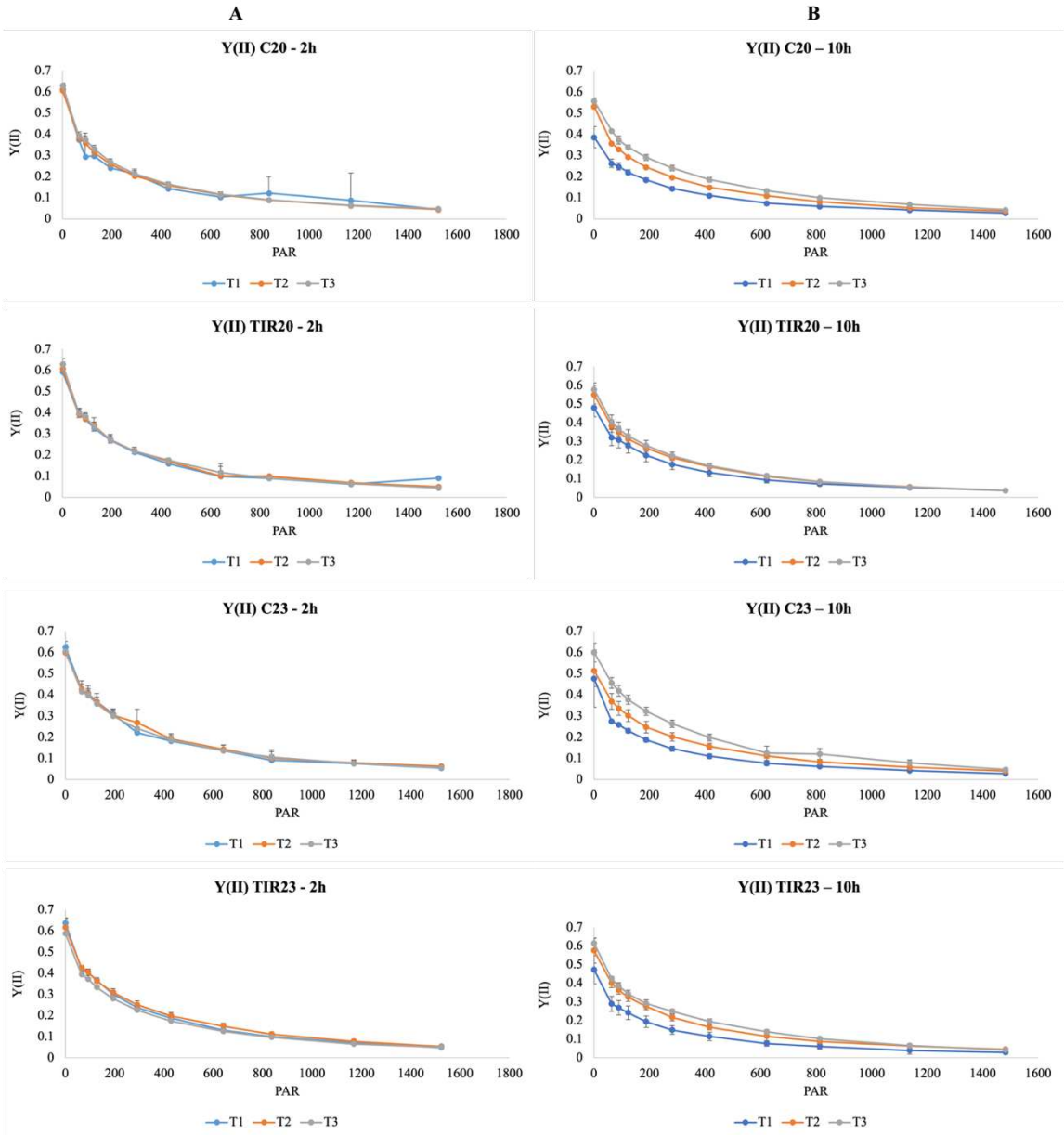

Figure 3.5 A) Y(II) values in time for C20, TIR20, C23 and TIR23 in the 2-h experiment; B) Y(II) values in time for C20, TIR20, C23 and TIR23 in the 10h-experiment

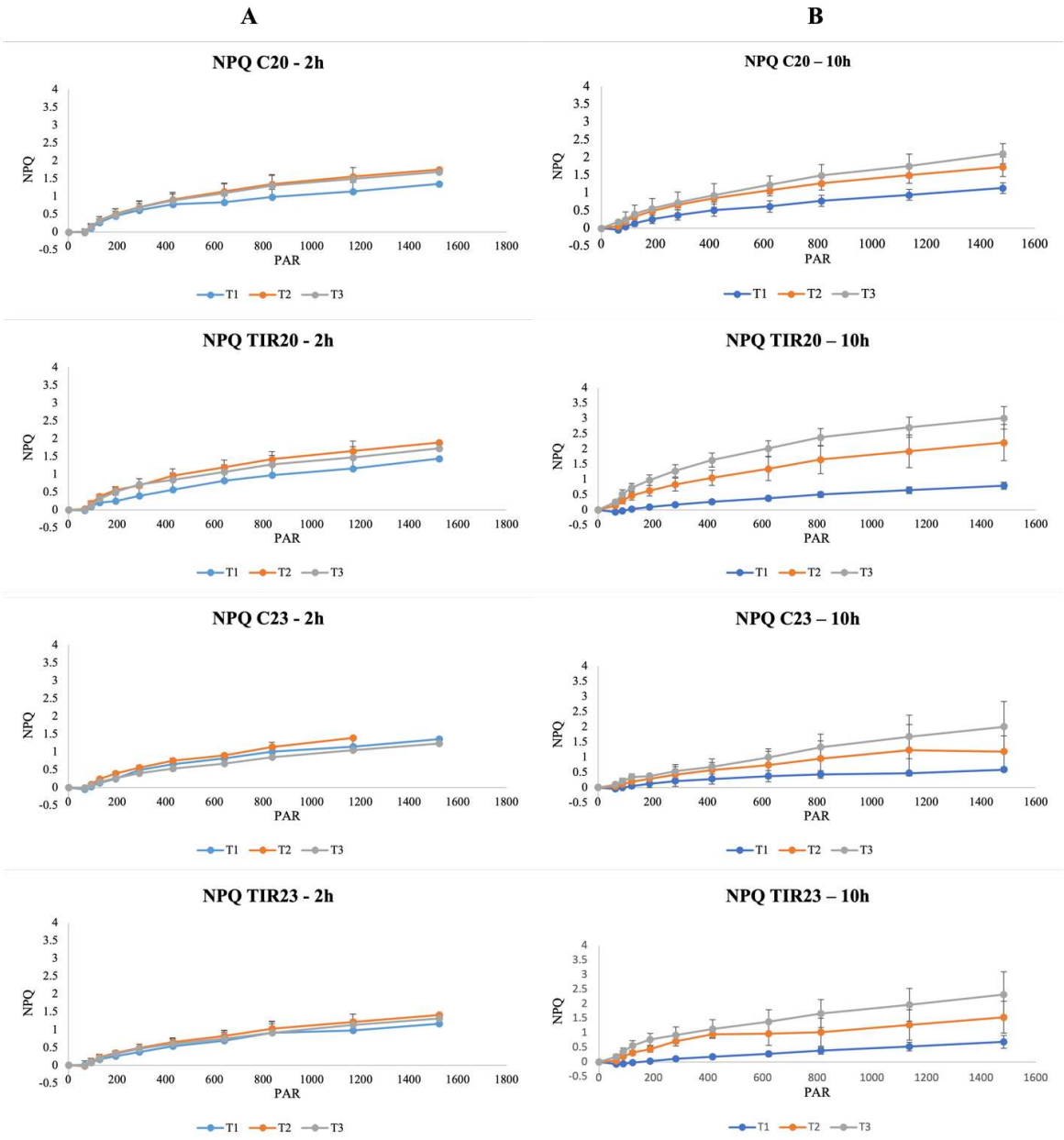

Figure 3.6 A) NPQ values in time for C20, TIR20, C23 and TIR23 in the 2-h experiment; B) NPQ values in time for C20, TIR20, C23 and TIR23 in the 10-h experiment

4. DISCUSSION

Photosynthetic unicellular algae and their host can be exposed to different light spectra, including far-red and near-infrared that penentrate deeper in the tissue of the coral and can be absorbed by chlorophylls or photoreceptors of the symbiont (Kosugi et al., 2024; Paradiso & Proietti, 2022; Smith et al., 2017), suggesting therefore that Symbiodiniaceae and their hosts can be affected by far-red and infra-red wavelengths.

Results from the 2-h experiments showed large differences in the measured variables, that might be linked to non-optimal rearing conditions. Moreover, PERMANOVA revealed very few variables significant, suggesting that the exposure time to the IR lamp is too short to be able to observe significant differences on the growth and photosynthetic rate of the symbiotic algae.

In the 10-h experiment, it is likely that the transfer from the source tank (water temperature 16°C) to the acclimation tank (water temperature 20°C) boosted the budding rate, highlighting that temperature is an important factor that might enhance or inhibit the asexual growth (Rodolfo-Metalpa et al., 2008). After acclimation, there were no significant variations in budding rates due to temperature or light quality.

Generally, high red irradiance (735 nm at an intensity of $2.0 Wm^{-2}$) inhibits the coral growth (Pulvinar-Camaya et al., 2016). In our experiments, the growth (increase in area and height of *C. caespitosa*) was not inhibited by the exposure to IR, the increase in area is likely related only to temperature, while changes in height could depend on both temperature and light quality.

At T1, the high concentration of symbionts (ranging from $1.5 \times 10^7 \pm 5.7 \times 10^6$ n cells gr^{-1} to $4.8 \times 10^7 \pm 3.3 \times 10^7$ n cells gr^{-1}) and the dark green color of the colonies can be considered indicators of good health conditions of *C. caespitosa* before the beginning of the experiment. However, the low values of Fv/Fm in T1 might be the results of a damage at the PSII of algae, meaning that the high irradiance in the experimental tanks could have affected the algae apparatus, reducing the photosynthetic efficiency. This could be due to a more rapid effect of irradiance on the photosynthetic efficiency than in the symbiotic cells (Murchie & Lawson, 2013) (Larkum et al., 2020).

In T2, it is likely that the high irradiance caused a ten-fold decline in the symbiont concentration and an evident bleaching of the living tissue. Notwithstanding the strong reduction in number, the algal cells observed in T2 and T3 were in good health conditions (no or a few broken cells were detected, doublet cells present) and the photosynthetic efficiency Fv/Fm increased respect to T1, suggesting that, after the severe effects of the intense light, the photosynthetic apparatus of the algal cells has been re-arranged and adapted to the new rearing conditions, underlying the high plasticity of *C. caespitosa* (Rodolfo-Metalpa et al., 2006).

PERMANOVA also recognized a significant increase in symbionts concentration in samples exposed to IR compared to their control at 23°C, contrasting the results from Wijgerde (2014) where they found less zooxanthellae in samples exposed to red light. These findings could suggest that IR could be beneficial, or at least not negative, to the acclimatation process.

Chlorophyll analysis revealed interesting differences in the ratio between the two main photopigment of the cell: chlorophyll-a and chlorophyll-c2 (Fig. 3.4C), indicating variations in the photosynthetic apparatus. Chlorophyll-a is found both in the reaction center and antenna pigments, while chlorophyll-c2 is only present in antenna proteins. A decline in chl-c2 might suggests a reduction in antenna pigments, possibly as a protective mechanism against excessive light, showed in the results as an increase in the ratio between chl-a and chl-c2 (Fig.3.4B, 10-h). In 15 days Scleractinians' symbionts acclimate by adjusting the chlorophyll-a and chlorophyll-c2 content per cell while maintain a constant ratio (Roth, 2014), coherent with the results obtained in 10-h experiment. In culture, however, the ratio varies under different light conditions, indicating that the host modulated the light environment for its symbiotic cells (Roth, 2014). Regarding the content of both chlorophyll-a and c2, it is possible to observe that the content of c2 is always lower than chlorophyll-a following the same pattern (Fig. 3.4A). The relationship between chlorophylls and symbionts concentration is negative, where we have a higher number of symbionts, we have a lower content in chlorophyll ($r = -0.5$). However, the indirect relationship revealed from the 10-h experiment could be explained as a process of photoacclimation of Symbiodiniaceae. It was revealed that when exposed to high irradiance, symbionts tend to regulate the abundance of chlorophyll-a rather than the accessory pigment: chlorophyll-a per

cell decreases with higher intensity (in nature this happens during summer, (Roth, 2014)), while with lower light intensity chlorophyll-a per cell tend to increase (Roth, 2014), a similar pattern obtained from the 10-h experiment.

The Y(II) results suggest that photosynthetic efficiency increased over time, likely due to the gradual acclimatation from the samples. The photoprotective mechanism for dissipating excess energy was analyzed through the trend of NPQ (Roth, 2014). NPQ increased in 10-h experiment, especially in the IR-exposed samples compared with their controls, possibly due to the difficulty in tolerating higher levels of irradiance. Activation and increase of NPQ is a normal process since corals can dissipate through NPQ approximately 96% of the total irradiance and only about 4% is used for photosynthesis (Roth, 2015). Overall, Y(II) and NPQ results indicate that sample maintained a certain efficiency in performing photosynthesis even thought the number of photosynthetic cells declined.

The coral skeleton can amplify the local light field, exacerbating the situation in cases of pigment or symbiont loss. Despite it has been observed some degree of bleaching occurring in most of the colonies, no direct impact on the photosynthetic apparatus was related to this effect (Roth, 2014). This could be explained by coral's ability to regulate pigment levels and gene expression to maintain optimal the conditions for the symbiont (Roth, 2014). Moreover, *C. caespitosa* can host different Symbiodiniaceae including *Breviolum psygmophilum*, which is very common in temperate waters and resistant to variations in temperature and light (Casado-Amezua et al., 2016) and, like other scleractinian, it is possible that the same colony of *C. caespitosa* can host multiple genera of Symbiodiniaceae while just one being the dominant one (La Jaunesse, 2002) (Rowan & Knowlton, 1995) making them able to better acclimate to different temperature and light conditions. In previous studies, *C. caespitosa* has been shown to tolerate short-term increases (32°C) and the tolerance is strongly dependent on the clade or genus of symbionts living in their tissue (e.g. *Cladocopium* is less tolerant to high temperature and light levels compared to *Symbiodinium* or *Breviolum*) (Rodolfo-Metalpa et al., 2006). In other experiments, it has been observed that the responses to light intensity, photoperiod and light spectra vary depending on the coral species, and therefore, are likely influenced by the species of Symbiodiniaceae (Izumi et al., 2023). On one hand, red light, particularly far-red light, alone acts as an inhibitor of growth, pigment content and zooxanthellae concentration (Wijgerde et al., 2014), while in other

species the trend is different. *Acropora tenuis* (Dana, 1846) shows higher growth when exposed to blue, red and violet light together compared to the absence of red spectrum light (Izumi et al., 2023). Similar trends have been found for zooxanthellae and chlorophyll content, where the concentration varies according to the species and the exposure to different light quantities and qualities (Izumi et al., 2023). *C. caespitosa* is known to be able at tolerating wide ranges of irradiances as well as temperatures and can rapidly acclimate. The acclimatation to high light intensities generally is characterized by an elevated NPQ which improve photoprotection, while the acclimatation to low light levels results in a decline of the photosynthetic parameters to maximize the capture of the low photon flux (Rodolfo-Metalpa, Huot, et al., 2008b). The capacity of acclimatation of *C. caespitosa* could explain, based on the results of this experiment, why the coral seems to gradually improve their conditions in every treatment, with light affecting symbionts, chlorophyll density and photoprotection mechanisms.

It is likely that *C. caespitosa* is able to survive in very shallow waters and to develop mechanisms to cope with high irradiance and IR light, at least in the Mediterranean waters, where intense solar radiation occurs at least at summertime (July-August).

5. CONCLUSIONS

From our knowledge, there are very few studies focused on the effect of corals and their photosynthetic symbionts to different light spectra such as UV, far-red FR or infrared IR (Wijgerde et al., 2014; Reynolds et al., 2008; Camaya et al., 2016; Izumi et al. 2022; Reef et al., 2009). For instance, the two experiment of this thesis offer more information and the starting point in exploring the effects on photosynthetic organism exposed to spectra of light that goes beyond the PAR. The results from samples exposed to only 2 hours on infrared did not show significant difference, probability due to the short time of exposure. The exposure to IR for 10 hours does not inhibit the coral's growth, conversely to what has been reported in previous studies (Wijgerde et al., 2014; Camaya et al., 2016) and it has been assess that increasing the water temperature (from 16°C to 20°C of the acclimatation tank) boosted the budding rate in all the samples. Moreover, IR may promote increase in colony height, but longer experiments should be performed to confirm our preliminary observations. Further studies are fundamental to better understanding how the host and their symbiotic photosynthetic cells reacts to this different wavelength. It would be important to reduce the light intensity in both PAR and PAR+IR tanks to avoid light-shocked and damaging the photosynthetic apparatus of the cells as well as trying to place the samples deeper in the tanks to favor their growth. A prolongate time of acclimatation could be essential to allow corals to better adapt to new conditions before the introduction of IR LED. Finally, for future studies it would be interesting to implement genetic studies in order to assess the genus of Symbiodiniaceae of *C. caespitosa* to see if its ability to adapt to wide range of temperature and light could be linked to a change in symbionts community, like it has been assessed to other Scleractinian (Rowan & Knowlton, 1995). Further investigation on the relationship between Symbiodiniaceae and *C. caespitosa* and their ability to adapt to different light conditions could provide insights into the resilience of the coral in a context of climate change, contributing to a better understanding of its survival.

APPENDIX

Colorimetric analysis of Cladocora caespitosa in 2-h

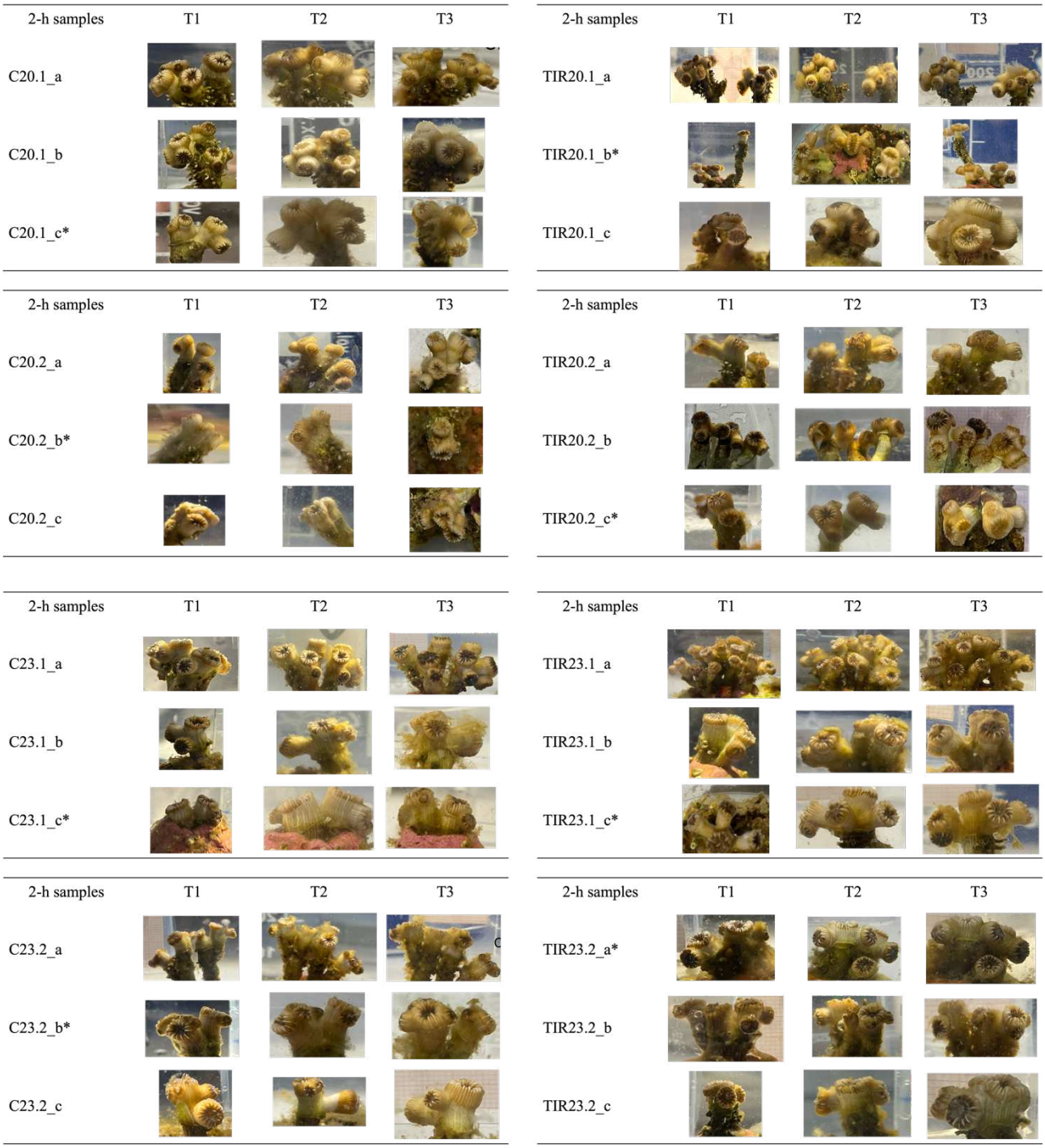

Figure 1 Bleaching analyses on Cladocora caespitosa in 2-h experiment

Colorimetric analysis of Cladocora caespitosa in 10-h

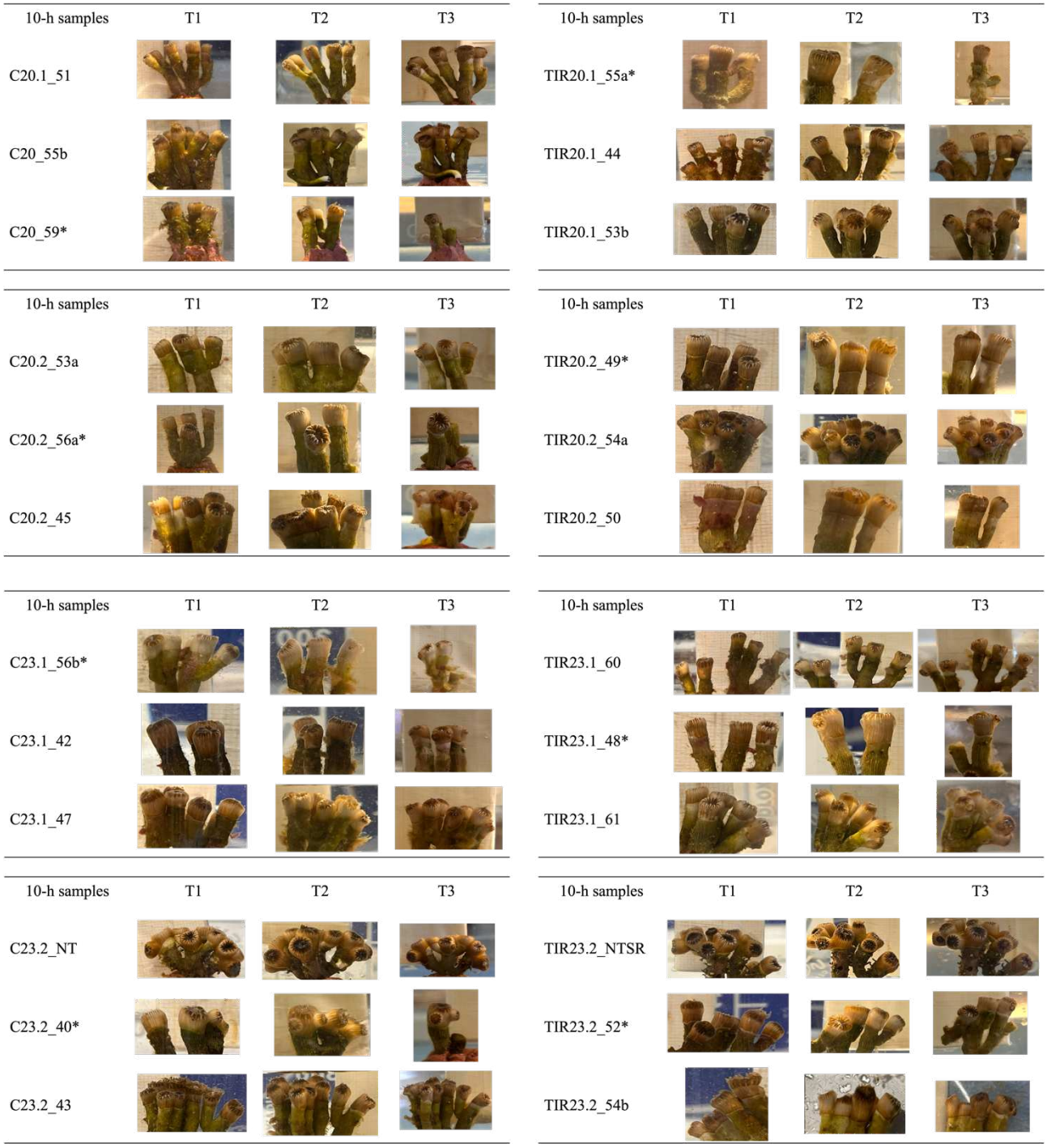

Figure 2 Bleaching analyses on Cladocora caespitosa in 10-h experiment

Bhagooli, R., & Hidaka, M. (2004). Photoinhibition, bleaching susceptibility and mortality in two scleractinian corals, Platygyra ryukyuensis and Stylophora pistillata, in response to thermal and light stresses. *Comparative Biochemistry and Physiology - A Molecular and Integrative Physiology*, *137*(3), 547–555. https://doi.org/10.1016/j.cbpb.2003.11.008

Bongaerts, P., Carmichael, M., Hay, K. B., Tonk, L., Frade, P. R., & Hoegh-Guldberg, O. (2014). Prevalent endosymbiont zonation shapes the depth distributions of scleractinian coral species. *Royal Society Open Science*, *2*(2). https://doi.org/10.1098/RSOS.140297

Bracchini, L., Cózar, A., Dattilo, A. M., Picchi, M. P., Arena, C., Mazzuoli, S., & Loiselle, S. A. (2005). Modelling the components of the vertical attenuation of ultraviolet radiation in a wetland lake ecosystem. *Ecological Modelling*, *186*(1), 43–54. https://doi.org/10.1016/J.ECOLMODEL.2005.03.001

Bucher, D. J., Harriott, V. J., & Roberts, L. G. (1998). Skeletal micro-density, porosity and bulk density of acroporid corals. *Journal of Experimental Marine Biology and Ecology*, *228*(1), 117–136. https://doi.org/10.1016/S0022-0981(98)00020-3

Bullerjahn, G. S., & Post, A. F. (1993). The prochlorophytes: Are they more than just chlorophyll a/b-containing cyanobacteria?? *Critical Reviews in Microbiology*, *19*(1), 43–59. https://doi.org/10.3109/10408419309113522

Casado de Amezua, P., Kersting, D., Linares, C. L., Bo, M., Caroselli, E., Garrabou, J., Cerrano, C., Ozalp, B., Terrón-Sigler, A., & Betti, F. (2015). *Cladocora caespitosa. The IUCN Red List of Threatened Species*.

Casado-Amezúa, P., Machordom, A., Bernardo, J., & González-Wangüemert, M. (2014). New insights into the genetic diversity of zooxanthellae in Mediterranean anthozoans. *Symbiosis* , *63*, 41–46. https://doi.org/10.1007/s13199-014-0286-y

Casado-Amezúa, P., Terrón-Sigler, A., Pinzón, J. H., Furla, P., Forcioli, D., Allemand, D., Ribes, M., & Coma, R. (2016). General ecological aspects of anthozoan- symbiodinium interactions in the mediterranean sea. *The Cnidaria, Past, Present and Future: The World of Medusa and Her Sisters*, 375–386. https://doi.org/10.1007/978-3-319-31305-4_24/FIGURES/6

Chefaoui, R. M., Casado-Amezúa, P., & Templado, J. (2017). Environmental drivers of distribution and reef development of the Mediterranean coral Cladocora caespitosa. *Coral Reefs*, *36*(4), 1195–1209. https://doi.org/10.1007/S00338-017-1611-8/FIGURES/6

Dall'Olio, L. R., Beran, A., Flander-Putrle, V., Malej, A., & Ramšak, A. (2022). Diversity of Dinoflagellate Symbionts in Scyphozoan Hosts From Shallow Environments: The Mediterranean Sea and Cabo Frio (Rio de Janeiro, Brazil). *Frontiers in Marine Science*, *9*, 867554. https://doi.org/10.3389/FMARS.2022.867554/BIBTEX

D'Angelo, C., Denzel, A., Vogt, A., Matz, M. V., Oswald, F., Salih, A., Nienhaus, G. U., & Wiedenmann, J. (2008). Blue light regulation of host pigment in reef-building corals. *Marine Ecology Progress Series*, *364*, 97–106. https://doi.org/10.3354/meps07588

Enríquez, S., Méndez, E. R., Hoegh-Guldberg, O., & Iglesias-Prieto, R. (2017). Key functional role of the optical properties of coral skeletons in coral ecology and evolution. *Proceedings of the Royal Society B: Biological Sciences*, *284*(1853). https://doi.org/10.1098/RSPB.2016.1667

Enríquez, S., Méndez, E. R., & Iglesias-Prieto, R. (2005). Multiple scattering on coral skeletons enhances light absorption by symbiotic algae. *Limnology and Oceanography*, *50*(4), 1025–1032. https://doi.org/10.4319/lo.2005.50.4.1025

European State of the Climate 2020 | Copernicus. (2020). https://climate.copernicus.eu/esotc/2020

Ferreira, G., Bollati, E., & Kühl, M. (2023). The role of host pigments in coral photobiology. In *Frontiers in Marine Science* (Vol. 10). Frontiers Media SA. https://doi.org/10.3389/fmars.2023.1204843

Galindo-Martínez, C. T., Chaparro, A., Enríquez, S., & Iglesias-Prieto, R. (2022). Modulation of the symbionts light environment in hospite in scleractinian corals. *Frontiers in Marine Science*, *9*. https://doi.org/10.3389/fmars.2022.1029201

Goulet, T. L., Cook, C. B., & Goulet, D. (2005). Effect of short-term exposure to elevated temperatures and light levels on photosynthesis of different host-symbiont combinations in the Aiptasia pallidal Symbiodinium symbiosis. *Limnology and Oceanography*, *50*(5), 1490–1498. https://doi.org/10.4319/LO.2005.50.5.1490

Hadjioannou, L., Jimenez, C., Rottier, C., Sfenthourakis, S., & Ferrier-Pagès, C. (2019). Response of the temperate scleractinian coral Cladocora caespitosa to high temperature and long-term nutrient enrichment. *Scientific Reports 2019 9:1*, *9*(1), 1–11. https://doi.org/10.1038/s41598-019-50716-w

Hill, R., Frankart, C., & Ralph, P. J. (2005). Impact of bleaching conditions on the components of non-photochemical quenching in the zooxanthellae of a coral. *Journal of Experimental Marine Biology and Ecology*, *322*(1), 83–92. https://doi.org/10.1016/J.JEMBE.2005.02.011

Hoogenboom, M., Beraud, • E, & Ferrier-Pagè, • C. (2009). Relationship between symbiont density and photosynthetic carbon acquisition in the temperate coral Cladocora caespitosa. *Coral Reefs*, *29*, 21–29. https://doi.org/10.1007/s00338-009-0558-9

Hoogenboom, M., Rodolfo-Metalpa, R., & Ferrier-Pagès, C. (2010). Co-variation between autotrophy and heterotrophy in the Mediterranean coral Cladocora caespitosa. *Journal of Experimental Biology*, *213*(14), 2399–2409. https://doi.org/10.1242/jeb.040147

Hughes, T. P. (1987). *Skeletal density and growth form of corals*. *35*, 259–266.

Kersting, D. K., Cefalì, M. E., Movilla, J., Vergotti, M. J., & Linares, C. (2023). The endangered coral Cladocora caespitosa in the Menorca Biosphere Reserve: Distribution, demographic traits and threats. *Ocean & Coastal Management*, *240*, 106626. https://doi.org/10.1016/J.OCECOAMAN.2023.106626

Kosugi, M., Ohtani, S., Hara, K., Toyoda, A., Nishide, H., Ozawa, S. I., Takahashi, Y., Kashino, Y., Kudoh, S., Koike, H., & Minagawa, J. (2024). Characterization of the far-red light absorbing light-harvesting chlorophyll a/b binding complex, a derivative of the distinctive Lhca gene family in green algae. *Frontiers in Plant Science*, *15*. https://doi.org/10.3389/FPLS.2024.1409116/FULL

Kružić, P., Žuljević, A., & Nikolić, V. (2008). Spawning of the colonial coral Cladocora caespitosa (Anthozoa, Scleractinia) in the Southern Adriatic Sea. *Coral Reefs*, *27*(2), 337–341. https://doi.org/10.1007/S00338-007-0334-7/FIGURES/5

Kühl, M., Trampe, E., Mosshammer, M., Johnson, M., Larkum, A. W. D., Frigaard, N. U., & Koren, K. (2020). Substantial near-infrared radiation-driven photosynthesis of chlorophyll f-containing cyanobacteria in a natural habitat. *ELife*, *9*. https://doi.org/10.7554/ELIFE.50871

LaJeunesse, T. C. (2002). Diversity and community structure of symbiotic dinoflagellates from Caribbean coral reefs. *Marine Biology*, *141*, 387–400. https://doi.org/10.1007/s00227-002-0829-2

LaJeunesse, T. C., Parkinson, J. E., Gabrielson, P. W., Jeong, H. J., Reimer, J. D., Voolstra, C. R., & Santos, S. R. (2018). Systematic Revision of Symbiodiniaceae Highlights the Antiquity and Diversity of Coral Endosymbionts. *Current Biology*, *28*(16), 2570-2580.e6. https://doi.org/10.1016/j.cub.2018.07.008

Lajeunesse, T. C., Parkinson, J. E., & Reimer, J. D. (2012). A genetics-based description of Symbiodinium minutum sp. nov. and S. psygmophilum sp. nov. (Dinophyceae), two

dinoflagellates symbiotic with cnidaria. *Journal of Phycology*, *48*(6), 1380–1391. https://doi.org/10.1111/J.1529-8817.2012.01217.X

LaJeunesse, T. C., Wiedenmann, J., Casado-Amezúa, P., D'Ambra, I., Turnham, K. E., Nitschke, M. R., Oakley, C. A., Goffredo, S., Spano, C. A., Cubillos, V. M., Davy, S. K., & Suggett, D. J. (2021). Revival of Philozoon Geddes for host-specialized dinoflagellates, 'zooxanthellae', in animals from coastal temperate zones of northern and southern hemispheres. *European Journal of Phycology*, *57*(2), 166–180. https://doi.org/10.1080/09670262.2021.1914863

Larkum, A. W. D., Grossman, A. R., & Raven, J. A. (2020). Photosynthesis in Algae: Biochemical and Physiological Mechanisms. In A. W. D. Larkum, A. R. Grossman, & J. A. Raven (Eds.), *Advances in Photosynthesis and Respiration* (Vol. 45). Springer International Publishing. https://doi.org/10.1007/978-3-030-33397-3

Legendre, R., & van Iersel, M. W. (2021). Supplemental Far-Red Light Stimulates Lettuce Growth: Disentangling Morphological and Physiological Effects. *Plants 2021, Vol. 10, Page 166*, *10*(1), 166. https://doi.org/10.3390/PLANTS10010166

Levy, O., Dubinsky, Z., & Achituv, Y. (2003). Photobehavior of stony corals: responses to light spectra and intensity. *Journal of Experimental Biology*, *206*(22), 4041–4049. https://doi.org/10.1242/JEB.00622

Marcelino, L. A., Westneat, M. W., Stoyneva, V., Henss, J., Rogers, J. D., Radosevich, A., Turzhitsky, V., Siple, M., Fang, A., Swain, T. D., Fung, J., & Backman, V. (2013). Modulation of Light-Enhancement to Symbiotic Algae by Light-Scattering in Corals and Evolutionary Trends in Bleaching. *PLoS ONE*, *8*(4). https://doi.org/10.1371/journal.pone.0061492

Mass, T., Kine, D. I., Roopin, M., Veal, C. J., Cohen, S., Iluz, D., & Levy, O. (2010). The spectral quality of light is a key driver of photosynthesis and photoadaptation in Stylophora pistillata colonies from different depths in the Red Sea. *Journal of Experimental Biology*, *213*(23), 4084–4091. https://doi.org/10.1242/JEB.039891

Meron, D., Rodolfo-Metalpa, R., Cunning, R., Baker, A. C., Fine, M., & Banin, E. (2012). Changes in coral microbial communities in response to a natural pH gradient. *The ISME Journal*, *6*, 1775–1785. https://doi.org/10.1038/ismej.2012.19

Murchie, E. H., & Lawson, T. (2013). Chlorophyll fluorescence analysis: A guide to good practice and understanding some new applications. In *Journal of Experimental Botany* (Vol. 64, Issue 13, pp. 3983–3998). https://doi.org/10.1093/jxb/ert208

Nitschke, M. R., Rosset, S. L., Oakley, C. A., Gardner, S. G., Camp, E. F., Suggett, D. J., & Davy, S. K. (2022). The diversity and ecology of Symbiodiniaceae: A traits-based review. *Advances in Marine Biology*, *92*, 55–127. https://doi.org/10.1016/BS.AMB.2022.07.001

Paradiso, R., & Proietti, S. (2022). Light-Quality Manipulation to Control Plant Growth and Photomorphogenesis in Greenhouse Horticulture: The State of the Art and the Opportunities of Modern LED Systems. *Journal of Plant Growth Regulation*, *41*(2), 742–780. https://doi.org/10.1007/S00344-021-10337-Y/TABLES/3

Pattison, P. M., Tsao, J. Y., Brainard, G. C., & Bugbee, B. (2018). LEDs for photons, physiology and food. *Nature 2018 563:7732*, *563*(7732), 493–500. https://doi.org/10.1038/s41586-018-0706-x

Pinho, P., Jokinen, K., & Halonen, L. (2017). The influence of the LED light spectrum on the growth and nutrient uptake of hydroponically grown lettuce. *Lighting Research and Technology*, *49*(7), 866–881. https://doi.org/10.1177/1477153516642269/ASSET/IMAGES/LARGE/10.1177_1477153516642269-FIG4.JPEG

Reynolds, J. M., Bruns, B. U., Fitt, W. K., & Schmidt, G. W. (2008). *Enhanced photoprotection pathways in symbiotic dinoflagellates of shallow-water corals and other cnidarians*. www.pnas.org/cgi/content/full/

Rodolfo-Metalpa, R., Huot, Y., & Ferrier-Pagès, C. (2008a). Photosynthetic response of the Mediterranean zooxanthellate coral Cladocora caespitosa to the natural range of light and temperature. *Journal of Experimental Biology*, *211*(10), 1579–1586. https://doi.org/10.1242/JEB.016345

Rodolfo-Metalpa, R., Huot, Y., & Ferrier-Pagès, C. (2008b). Photosynthetic response of the Mediterranean zooxanthellate coral Cladocora caespitosa to the natural range of light and temperature. *Journal of Experimental Biology*, *211*(10), 1579–1586. https://doi.org/10.1242/JEB.016345

Rodolfo-Metalpa, R., Peirano, A., Houlbrèque, F., Abbate, M., & Ferrier-Pagès, C. (2008). Effects of temperature, light and heterotrophy on the growth rate and budding of the temperate coral Cladocora caespitosa. *Coral Reefs*, *27*(1), 17–25. https://doi.org/10.1007/s00338-007-0283-1

Roveta, C., Coppari, M., Calcinai, B., Di Camillo, C. G., Marrocco, T., Pulido Mantas, T., Puce, S., Torsani, F., Valisano, L., & Cerrano, C. (2023). What's the key for success? Translocation,

growth and thermal stress mitigation in the Mediterranean coral Cladocora caespitosa (Linnaeus, 1767). *Frontiers in Marine Science*, *10*. https://doi.org/10.3389/fmars.2023.1199048

Rowan, B., & Knowlton, N. (1995). Intraspecific diversity and ecological zonation in coral-algal symbiosis. *Proceedings of the National Academy of Sciences of the United States of America*, *92*(7), 2850–2853. https://doi.org/10.1073/PNAS.92.7.2850

Salih, A., Larkum, A., Cox, G., Kühl, M., & Hoegh-Guldberg, O. (2000). Fluorescent pigments in corals are photoprotective. *Nature 2000 408:6814*, *408*(6814), 850–853. https://doi.org/10.1038/35048564

Sinanoglou, V. J., Kavga, A., Strati, I. F., Sotiroudis, G., Lantzouraki, D., & Zoumpoulakis, P. (2019). Effects of Infrared Radiation on Eggplant (Solanum melongena L.) Greenhouse Cultivation and Fruits' Phenolic Profile. *Foods 2019, Vol. 8, Page 630*, *8*(12), 630. https://doi.org/10.3390/FOODS8120630

Smith, E. G., Angelo, D. D. ', Sharon, C., Tchernov, Y., & Wiedenmann, D. (2017). *Acclimatization of symbiotic corals to mesophotic light environments through wavelength transformation by fluorescent protein pigments*. https://doi.org/10.1098/rspb.2017.0320

Sorek, M., & Levy, O. (2012). Influence of the Quantity and Quality of Light on Photosynthetic Periodicity in Coral Endosymbiotic Algae. *PLoS ONE*, *7*(8), 43264. https://doi.org/10.1371/JOURNAL.PONE.0043264

Stambler, N., & Dubinsky, Z. (2005). Corals as light collectors: An integrating sphere approach. *Coral Reefs*, *24*(1), 1–9. https://doi.org/10.1007/s00338-004-0452-4

Terán, E., Méndez, E. R., Enríquez, S., & Iglesias-Prieto, R. (2010). *Multiple light scattering and absorption in reef-building corals*.

Titlyanovl, E. A., Titlyanoval, T. V, Tsukahara2, J., Van Woes1k3, R., & Yamazatq4, K. (1999). Experimental Increases of Zooxanthellae Density in the Coral Stylophora pistillata Elucidate Adaptive Mechanisms for Zooxanthellae Regulation. *Symbiosis*, *26*, 347.

Visram, S., Wiedenmann, J., & Douglas, A. E. (2006). Molecular diversity of symbiotic algae of the genus Symbiodinium (Zooxanthellae) in cnidarians of the Mediterranean Sea. *Journal of the Marine Biological Association of the United Kingdom*, *86*(6), 1281–1283. https://doi.org/10.1017/S0025315406014299

Wangpraseurt, D., Jacques, S. L., Petrie, T., & Kühl, M. (2016). Monte Carlo modeling of photon propagation reveals highly scattering coral tissue. *Frontiers in Plant Science*, *7*(September). https://doi.org/10.3389/fpls.2016.01404

Wangpraseurt, D., Larkum, A. W. D., Franklin, J., Szabo, M., Ralph, P. J., & Kuhl, M. (2014). Lateral light transfer ensures efficient resource distribution in symbiont-bearing corals. *Journal of Experimental Biology*, *217*(4), 489–498. https://doi.org/10.1242/jeb.091116

Wangpraseurt, D., Larkum, A. W. D., Ralph, P. J., & Kühl, M. (2012). Light gradients and optical microniches in coral tissues. *Frontiers in Microbiology*, *3*(AUG). https://doi.org/10.3389/fmicb.2012.00316

Wangpraseurt, D., Tamburic, B., Szabó, M. N., Suggett, D., Ralph, P. J., & Kü Hl, M. (2014). Spectral effects on Symbiodinium photobiology studied with a programmable light engine. *PLoS ONE*, *9*(11). https://doi.org/10.1371/journal.pone.0112809

Widiarti, R., Johan, O., & Fadillah, M. F. (2016). Effect Of Light Intensity To The Abundance Of Zooxanthellae On Large Polyp Stony Corals At Panggang Island Waters, Based On Depth Differences. *International Seminar Sustainable Utilization of Coastal Resources in Tropical Zones*. https://www.researchgate.net/publication/319504145

Wijgerde, T., Van Melis, A., Silva, C. I. F., Leal, M. C., Vogels, L., Mutter, C., & Osinga, R. (2014). Red light represses the photophysiology of the scleractinian coral Stylophora pistillata. *PLoS ONE*, *9*(3). https://doi.org/10.1371/journal.pone.0092781

Y. Loya, K. S. K. Y. Y. N. H. S. and R. van W. (2001). Coral bleaching: the winners and the losers. *Ecology Letter*, 122–131. https://doi.org/10.1046/j.1461-0248.2001.00203.x

Yellowlees, D., Rees, T. A. V., & Leggat, W. (2008). Metabolic interactions between algal symbionts and invertebrate hosts. *Plant, Cell & Environment*, *31*(5), 679–694. https://doi.org/10.1111/J.1365-3040.2008.01802.X

Zhou, J., Huang, H., Beardall, J., & Gao, K. (2017). Effect of UV radiation on the expulsion of Symbiodinium from the coral Pocillopora damicornis. *Journal of Photochemistry and Photobiology B: Biology*, *166*, 12–17. https://doi.org/10.1016/j.jphotobiol.2016.11.003